

# The Multiverse, the Milky Universe, and the Periodic Table of Elementary Particles

Ding-Yu Chung\*

All leptons, quarks, and gauge bosons can be placed in the periodic table of elementary particles. The calculated masses for elementary particles and hadrons are in good agreement with the observed masses. For examples, the calculated masses for the top quark and neutron are 176.5 GeV and 939.54MeV in agreement with the observed masses, 174.3 GeV and 939.57 MeV, respectively. The periodic table consists of two sets of seven orbitals, which can be explained by the two sets of seven extra dimensions from the combination of two eleven dimensional universes, implying the multiverse. The multiverse consists of varying dimensions from varying speed of light and varying object-space. The multiverse explains the inflation, the big bang, the cyclic universe, renormalization, quantum mechanics, and dark energy. The cosmic evolution based on the multiverse generates dark matter as six particles from 5D to 10D and baryonic matter as one 4D-particle, which have the mass ratio of 6/1 as observed. Due to the structural difference, baryonic matter and dark matter are incompatible to each other as oil and water in emulsion (milk), resulting in the “Milky Universe”. This Milky Universe explains the evolution of galaxies, anisotropies in the CMB, and MOND. Therefore, the cosmic evolution takes place in the multiverse, we live in the Milky Universe, and our baryonic matter follows the periodic table of elementary particles. This whole picture of Nature provides viable cosmology, detailed explanation of astronomy, and accurate calculation of the masses of elementary particles and hadrons.

## Introduction

All leptons, quarks, and gauge bosons can be placed in the empirical periodic table of elementary particles [1]. The calculated masses for elementary particles and hadrons are in good agreement with the observed masses. The accurate calculation for the masses of elementary particles first appeared in the quantized lepton mass formula by A.O. Barut [2].

$$M_n = M_e + \frac{3}{2} M_e \alpha \sum_{n=0}^n n^4$$

where  $n = 0, 1,$  and  $2$  for electron, muon, and  $\tau$ , respectively. The calculated masses 105.5 and 1786 MeV for muon and  $\tau$ , respectively, in good agreement with the observed masses, 105.7 and 1777 MeV. The quantized lepton mass formula indicates the orbital structure.

The lepton mass formula was expanded to calculate the masses of all leptons, quarks, and gauge bosons [1]. The calculation involves only two simple mass formulas (Eq. (11) for gauge bosons and Eq. (19) for leptons and quarks) and only four constants (the fine structure

constant, the mass of electron, the mass of  $Z^0$ , and a pair of seven orbitals). The masses of elementary particles are periodic, and can be expressed in the forms of the periodic table of elementary particles (Table 2). The periodic table of elementary particles forms the base for M. H. MacGregor's constituent quark model [3] that calculates the masses of hadrons accurately.

The periodic table of elementary particles has the orbital structure (Fig. 17) containing two sets of seven orbitals. These two sets of seven orbitals can be explained by the two sets of seven extra dimensions from the combination of two eleven dimensional universes, implying the multiverse. The multiverse consists of two variable components: varying dimensions from varying speed of light and varying object-space. Different universes in the multiverse have different variables from these two variable components.

The cosmic evolution based on the multiverse generates six mass dimensional particle matters from 5D to 10D and one 4D-particle matter, corresponding to dark matter and baryonic matter with the mass ratio of 6/1 as observed. Due to the structural difference, baryonic matter and dark matter are incompatible to each other as oil and water in emulsion (milk), resulting in the "Milky Universe". Therefore, the cosmic evolution takes place in the multiverse, we live in the Milky Universe, and our baryonic matter follows the periodic table of elementary particles.

The paper is divided into three parts: the multiverse, the Milky Universe, and the periodic table of elementary particles. Section 1 describes varying space-time dimensions and varying mass dimensions. Section 2 describes the evolution of the expanding universe and object-space. The cosmic expansion mechanism and the two different modes of the cosmic expansion are described in Section 3. The derivation of quantum mechanics is described in Section 4. In Section 5, the cyclic universe is proposed. The formation of inhomogenous structure in the observable universe based on the Milky Universe is described in Section 6. The evolution of galaxies is stated in Section 7. In Sections 8, 9 and 10, the periodic table of elementary particles is constructed to account of all leptons, quarks, gauge bosons, and hadrons, and their masses are calculated.

## **Part 1: The Multiverse**

### ***1. Varying Space-time Dimensions and Varying Mass Dimensions***

The multiverse consists of two variable components: varying dimensions and varying object-space. Different universes in the multiverse have different compositions of variables from the two variable components. Varying dimensions are derived from varying speed of light (VSL) theory [4].

In VSL theory, the speed of light varies with its frequency, with higher speeds for higher frequencies and energies. In this paper, there are both varying speed of light and varying space-time dimension. The varying speed of light is quantized by varying space-time dimension as follows.

$$c_D = c / \alpha^{D-4}, \quad (1)$$

where  $c_D$  is the quantized varying speed of light in space-time dimension,  $D$ , which is the Kaluza-Klein space-time dimension from 4 to 11. The speed of light in the four dimensional space-time is  $c$ , and  $\alpha$  is the fine structure constant. Each space-time dimension has a specific speed of light. The speed of light increases with increasing space-time dimension number,  $D$ . In relativity,  $E = M_0 c^2$  modified by Eq. (1) is expressed as

$$E = M_0 (c^2 / \alpha^{2(D-4)}) \quad (2a)$$

$$= (M_0 / \alpha^{2(D-4)}) c^2 \quad (2b)$$

Eq. (2a) means that a particle in the  $D$  dimensional space-time can have superluminal speed,  $c / \alpha^{D-4}$ , that is higher than the normal speed of light, and has rest mass,  $M_0$ . Eq. (2b) means that the same particle in the four-dimensional space-time with the normal speed of light acquires  $M_0 / \alpha^{2(D-4)}$  as the rest mass.  $D$  in Eq. (2a) is space-time dimension defining the varying speed of light.  $D$  from 4 to 11 in Eq. (2b) is “mass dimension” defining varying mass. For example, for  $D = 11$ , Eq. (2a) shows a superluminal particle in eleven-dimensional space-time, while Eq. (2b) shows that the space-time dimension of same particle is four, and the mass dimension is eleven. Therefore, in relativity, quantized varying speed of light in terms of varying space-time dimension,  $D$ , brings about varying mass in terms of varying mass dimension,  $D$ .

According to Eq. (2), at the same total energy, the rest mass increases with decreasing space-time dimension,

$$M_{0,D} = M_{0,D-1} \alpha^2 \quad (3)$$

where  $D$  is space-time dimension from four to eleven. The four-dimensional space-time has the lowest space-time dimension, so its maximum rest mass is the highest mass, the Planck mass, and its maximum mass dimension is the highest mass dimension,  $D_{\max}, 11$ . In the 11-dimensional space-time as the highest space-time dimension, the maximum mass dimension is 4. Therefore, for each space-time dimension,  $D$ ,

$$D_{\max,D} = 15 - D \quad (4)$$

where  $D_{\max}$  is the maximum mass dimension. A decrease in  $D$  leads to an increase in  $D_{\max}$ .

As space-time dimension, vacuum energy (a scalar field) decreases with increasing rest mass, so vacuum energy can be defined by space-time dimension and the speed of light. In the four-dimensional space-time as the lowest space-time dimension, vacuum energy is zero.

In the same dimensional space-time, a particle can transform (fractionalize or condense) into particles with mass dimensions  $\geq 4$  and  $\leq D_{\max}$ . For example, a particle with 4-dimensional space-time can transform into the particles with mass dimensions from 4 up to 11. The transformation is through “varying supersymmetry”. In the normal supersymmetry, the repeated application of the fermion-boson transformation transforms a boson (or fermion) from one point to the same boson (or fermion) at another point at the

same mass. In the “varying supersymmetry”, the repeated application of the fermion-boson transformation transforms a boson from one point to the boson with different mass at another point at different mass dimension. The repeated varying supersymmetry transformation transforms boson  $B_D$  into fermion  $F_D$  and from fermion  $F_D$  to boson  $B_{D-1}$  is expressed as

$$M_{D,F} = M_{D,B} \alpha_{D,B}, \quad (5a)$$

$$M_{D-1,B} = M_{D,F} \alpha_{D,F}, \quad (5b)$$

where  $M_{D,B}$  and  $M_{D,F}$  are the masses for a boson and a fermion, respectively,  $D$  is mass dimension, and  $\alpha_{D,B}$  or  $\alpha_{D,F}$  is the fine structure constant, which is the ratio between the masses of a boson and its fermionic partner. Assuming  $\alpha_{D,B} = \alpha_{D,F}$ , the relation between the bosons in the adjacent dimensions, then, can be expressed as

$$M_{D-1,B} = M_{D,B} \alpha^2_D, \quad (5c)$$

which means that under varying supersymmetry, a particle moves and changes mass at the same time. The dimensional masses, therefore, can be calculated for all mass dimensions by Eq. (5), which is verified empirically later [2].

## 2. *From the Pre-universe to the Expanding Universe: Variable Object-Space*

Another variable component of the multiverse is object-space component consisting of four objects and four spaces. Objects has definite shapes, and spaces are homogeneous. Objects include string, membrane, particle, and particle-wave. Spaces include blank space, fermion space, boson space, and exclusion space. Blank space takes turn to coexist equally with object at the same location as in creation and annihilation of particle in vacuum. Fermion space exists with an object at the same location or different locations in one object to one space relation as in fermion. Boson space exists at the same location with multiple objects as in boson. Exclusion space excludes object at the same location as the space of traveling light in the sense that light is forced to travel by permanent exclusion of space by exclusion space.

The evolution of our expanding universe involves four stages: the pre-universe, the pre-expanding universe, the mixed pre-expanding universe, and the expanding universe. Different stages of evolution have different compositions of variables from varying space-time dimensions and varying object-space.

The starting multiverse (the pre-universe) is essentially a homogeneous blank consisting of  $10D$  superstring in equilibrium with vacuum at a non-zero vacuum energy and superluminal speed. The pre-universe is blank space-object, the equilibrium state between the vacuum and the pairs of ten-dimensional superstring and anti-superstring. The vacuum energy is equal to the non-zero energy of the superstring. The pre-universe is the platform for the multiverse.

Blank space can also undergoes vacuum fluctuation as condensation and diffusion. The condensation as the compactification of higher dimensions leads to the formation of a two space-time dimensional string and the empty space as fermion space, each of which associates with one object. One object per space is the definition of fermion.

The compact two space-time dimensional string has the Planck mass. This  $2D$  string attaches to the  $10D$  superstring to provide the eleventh dimension for an eleven-dimensional membrane as Fig. (1). The compact string has the Planck mass. The pre-universe is pre-quantum mechanics without uncertainty, so without uncertainty, the space-time of the  $2D$ -string attaches to the space-time of the adjacent  $10D$ -superstring precisely. This evolution from string to membrane is the reverse of M-theory that starts with  $11D$ -membrane.

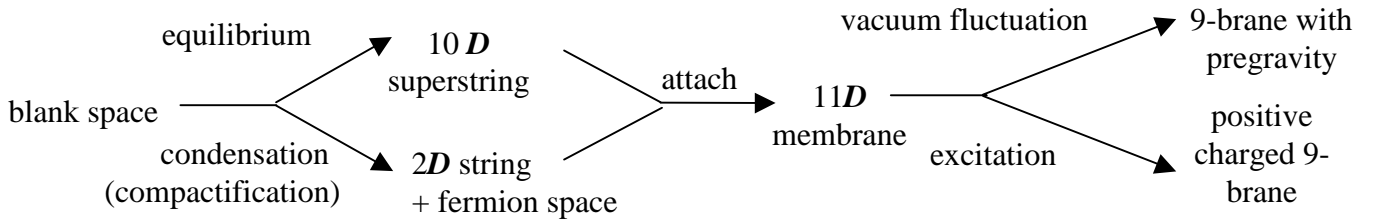


**Fig. 1:** the evolution of 9-brane in the pre-expanding universe

The attached string can undergo vacuum fluctuation and excitation. In terms of vacuum fluctuation, the non-zero vacuum energy causes the attached string to diffuse into fermion space to become an infinite dimension. Subsequently, the attachment of the string in membrane provides AdS (anti-de Sitter space) for the diffused string to condense (compactify) again. When this diffusion-condensation overlaps with the diffusion-condensation from another membrane, "pregravity" (the predecessor of gravity) is formed. Pregravity is in boson space that allows more than multiple objects per space. Boson is defined as multiple objects per space. This diffusion-condensation reproduces the Planck-infinite dimension in the Randall-Sundrum model [5] for gravity. The resulting structure is 9-brane ( $10D$ -brane) embedded in the eleven-dimensional bulk with pregravity. Since pregravity is active in an empty space, pregravity is a long-ranged force as Fig. 1 and Fig. 2.

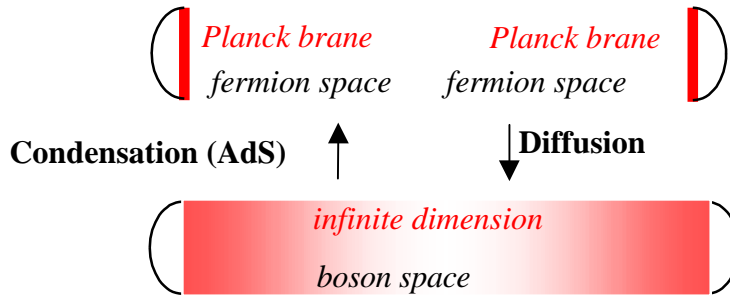


**Fig. 2:** pregravity as the Randall-Sundrum model

In terms of excitation, the attached string behaves as the  $1D$  circle circling superstring in the  $10D \times 1D$  Kaluza-Klein structure. The quantized excitation of the circle brings about the quantized positive pre-charged force (the predecessor of electromagnetism) with the absorption and the emission of the massless particles in exchange with the massless particles from other membranes. Since the pre-charged force is active in empty space, the pre-charged force is a long-ranged force as Fig. 1 and Fig. 3.

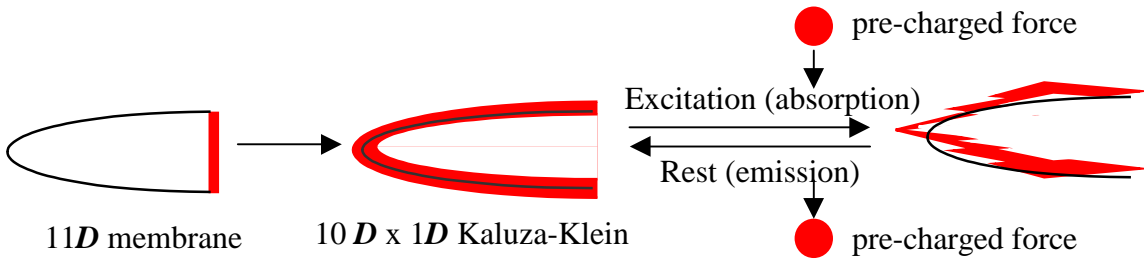


**Fig. 3:** pre-charged force from excitation

The combination of the vacuum fluctuation and the excitation of the attached string results in the positive charged 9-brane embedded in the eleven-dimensional bulk with pregravity and positive pre-charged force (Fig. 1). At the same time, the ten-dimensional anti-superstring becomes negative charged 9-antibrane embedded in the eleven-dimensional bulk with anti-pregravity and negative pre-charged force.

The original force among strings in the pre-universe is the pre-strong force, the predecessor of the strong force. The force is resulted from the absorption and the emission of massless particles from strings. Since it transmits through blank space with non-zero energy, rather than an empty space, it is a short-ranged force through a non-zero energy medium. This pre-strong force remains as a short-ranged force among membranes.

The combination of the 9-brane and the 9-antibrane is the brane-antibrane unit. The structure of the brane-antibrane unit is determined by the evolutionary sequence of the three forces. In the normal evolutionary sequence, the pre-strong force exists first. Then, the emergence of the repulsive force between pregravity and anti-pregravity forces a brane and an antibrane to move away from each other. Subsequently, the pre-strong force connects the newly formed brane or the antibrane with previously formed branes or antibranes. Finally, the pre-charged force emerges. The space occupied by branes is

opposite from the space occupied by antibranes, so branes and antibranes are chiral. This normal evolutionary sequence provides the chiral brane-antibrane unit where the chiral boundary positive charged 9-brane and the chiral boundary negative charged 9-antibrane embedded in the eleven-dimensional space-time are separated by chiral pregravity and chiral anti-pregravity as Fig. 4.

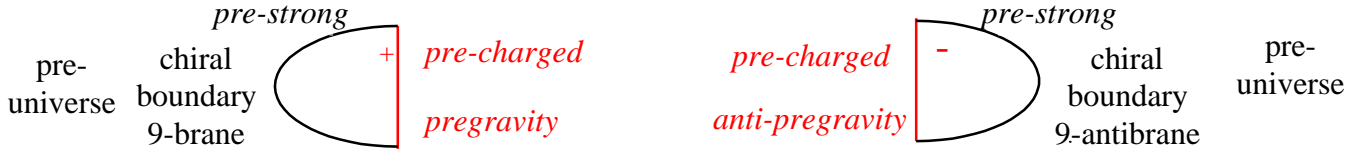


**Fig. 4:** the pre- expanding universe

The pre-expanding universe emerges with this chiral brane-antibrane unit as the predominant structure. All forces and membranes inside the pre-expanding universes are chiral. The pre-expanding universe continues to grow with the conversion of the pre-universe vacuum entering into the fermion space in the middle of the pre-expanding universe. This two-brane structure of the pre-expanding universe also appears in the Horava-Witten eleven dimensional pregravity on a manifold with two ten-dimensional boundaries [6], the ekpyrotic universe boundary branes [7], and the brane-antibrane universe [8].

During the steady conversion from the pre-universe to the pre-expanding universe takes place, the total volume of the two universes remain constant. To maintain this constant volume, the attractive force (A) between the positive and negative pre-charged forces is equal to the sum of the repulsive force (R) between pregravity and anti-pregravity, and the special global short-ranged pre-strong force (C) connecting the pre-expanding universe and the pre-universe.  $A = R + C$  is a non-localized global relation for the constant total volume of the universes. If  $A > R + C$ , the total volume is smaller, and if  $A < R + C$ , the total volume is larger.

There is a small amount of the abnormal evolutionary sequence in the pre-expanding universe. In the abnormal evolutionary sequence, the pre-strong force exists first. Then, the emergence of the attractive force from the pre-charged forces draws the brane and the antibrane together. The combined brane-antibrane units go impartially to either side of the pre-expanding universe, resulting in the achiral brane-antibrane units. (Essentially, attractive force and repulsive force are the tools to form chirality and achirality.) Finally, pregravity and anti-pregravity emerge. In the universe, local interactions are either chirality-specific or achirality-specific. Unable to interact with the region inside the chiral pre-expanding universe, the achiral brane-antibrane units are separated from the chiral pre-expanding universe, and congregate in the area connecting the pre-universe and the pre-expanding universe. The result is the decrease of the connection between the pre-expanding universe and the pre-universe. However, as a non-localized global relation,  $A = R + C$  continues with the right amount of C contributed by the pre-universe as long as there is still connection between the pre-universe and the pre-expanding universe.

As the pre-expanding universe grows with the chiral brane-antibrane units, the number of the achiral brane-antibrane units grows. Eventually, the pre-expanding universe is disconnected completely from the pre-universe by the achiral brane-antibrane units. Without C, the excess attractive force ( $A > R$ ) between positive branes and negative charged antibranes causes the pre-expanding universe to collapse, and the repulsive force between pregravity and anti-pregravity causes the pre-expanding universe to inverse. As the 9-brane and the 9-antibrane move toward each other, the 9-brane and the 9-antibrane turn inside, and pregravity and anti-pregravity turn outside. The "gulf" separating the pre-expanding universe and the pre-universe is formed. Eventually, the 9-brane and the 9-antibrane coalesce. At the end of the coalescence, the repulsion between pregravity and anti-pregravity causes a bounce after the collapse.

At this point, the complete coalescence leads to the loss of the properties of brane and antibrane in terms of the membrane property, the pre-charged force, the pre-strong force, and chirality. The result is the generation of the achiral mixed 9-particle with the multiple dimensional Kaluza-Klein structure without the requirements for identical space dimensions and a fixed number of space dimensions as in superstring. All forces formed previously become achiral. The bounce results in the mixed pre-expanding universe, consisting of four equal parts: two groups of achiral mixed 9-particles, achiral pregravity, and achiral anti-pregravity as Fig. 5.

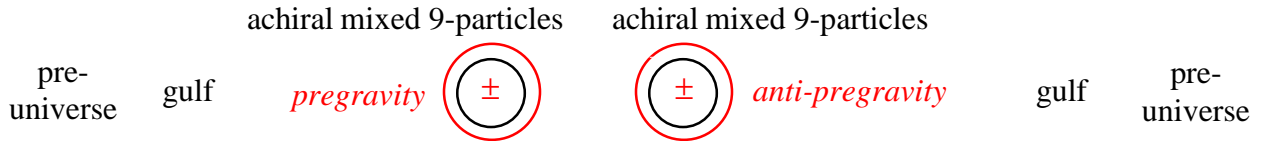


**Fig. 5:** the mixed pre-expanding universe

The interactions between branes in the form of collision are proposed in various brane models [7, 8, 9]. The cyclic universe model based on the ekpyrotic universe [10] has the collapse-singularity-bounce scheme.

The size of the pre-expanding universe is determined by the ratio between the number of the chiral units and the number of the achiral units. The pre-universe and the mixed pre-expanding universe are different in the composition of objects and spaces, and are separated from each other permanently. Consequently, the two universes are completely transparent to each other. Without relation with the pre-universe, the mixed pre-expanding universe has its own vacuum energy that decreases from the non-zero in the pre-universe to zero. With decreasing vacuum energy and the Kaluza-Klein structure without a fixed number of space dimensions, the space-time dimension and the mass dimension of mixed 9-particles decrease to lower dimensional space-time and lower dimensional mass. The decrease to lower mass dimension results in the fractionalization of mixed 9-particles into lower mass particles, leading to the expansion of the universe. The fractionalization leads to the cosmic expansion into the completely transparent pre-universe. It is the start of the expanding universe. To the pre-universe, the expanding universe is a missing region.



### 3. *The Expanding Universe: the Hidden Universe and the Observable Universe*

The cosmic expansion in terms of the fractionalization of 9-mixed particles involves two different modes for the two sides of the expanding universe: the slow mode for the hidden universe and the quick mode for the observable universe as Fig. 6.

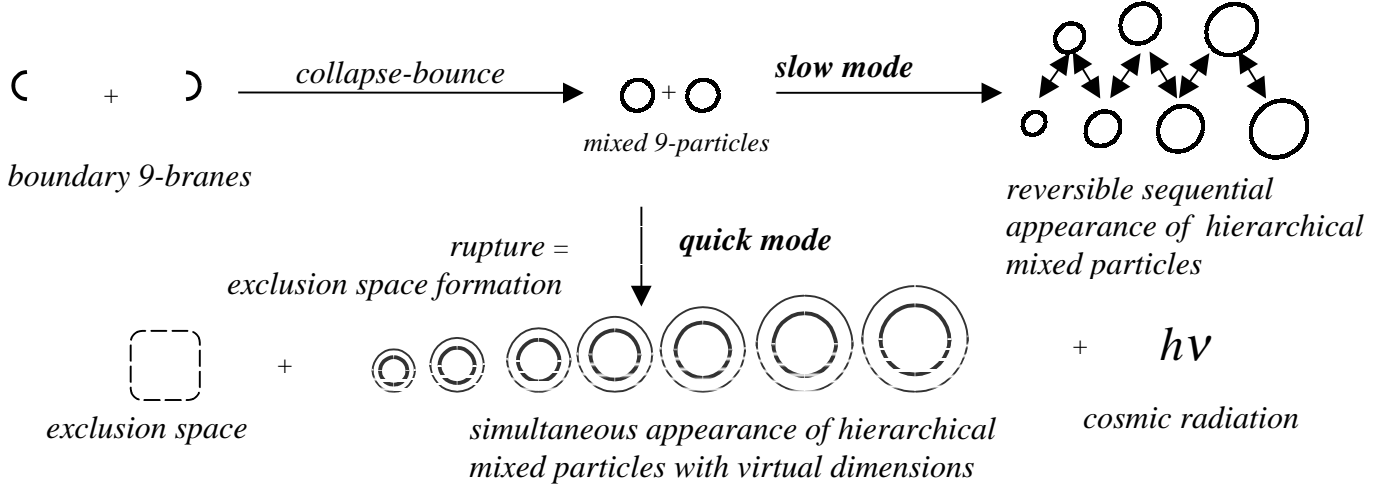


**Fig. 6:** the slow mode and the quick mode

The slow mode is used in the hidden universe. In the slow mode, the vacuum energy decreases to zero gradually, and the space-time dimension of the  $10D$  mixed particle with gravity decreases from  $10D$  to  $4D$ , sequentially. The decrease in vacuum energy leads to the decrease in space-time dimension ( $D \rightarrow D - 1$ ) and the increase in the rest mass ( $D \rightarrow D + 1$ ). The rest mass is fractionalized through varying supersymmetry until  $D = 4$ . Such varying supersymmetrical transformation brings about the translational movement (expansion). Further decrease in vacuum energy repeats the same process again until all particles are the  $4D$  particles. At the end of the cosmic expansion, the universe undergoes the slow condensation back to the  $10D$  particle with the increase in space-time dimension sequentially. The hidden universe undergoes expansion and contraction as the top figure in Fig. 6.

The quick mode is used in the observable universe. In the quick mode, the vacuum energy decreases immediately to zero with  $4D$  space-time, resulting in the  $4D$  (four space-time dimensional)  $10D$  (ten mass dimensional) particles. The  $10D$  particles immediately fractionalize into the mixture of particles with different mass dimensions from  $4D$  to  $10D$ . The mechanism for the immediate fractionalization is renormalization by exclusion space.

In renormalization, mass dimensions are divided into real mass dimensions for real particles with mass-charge and virtual mass dimensions for virtual particles. Different real particles occupy different real mass dimensions, resulting in the immediate fractionalization into the mixture of particles with different mass dimensions from  $4D$  to  $10D$  in seven equal mass portions as shown in the bottom figure in Fig. 6. For example, for the  $4D$  particle (baryonic matter) at the ground state, the real particle with real mass-

charge occupies the first four mass dimensions, while the virtual particle occupies the rest of the mass dimensions. (The particles from 5D to 10D are dark matter as shown later.)

The interaction between real and virtual particles results in finite increase in mass and charge, if the interaction follows the well-defined mass dimensions. When the interaction, such as loops (pairs of particle and anti-particle) in Feynman diagrams, is independent of and potentially deviates from the mass dimensions, mass-charge without the restriction of the mass dimensions becomes infinite ( $D \rightarrow \infty$ ).

To avoid the infinite physical mass and charge, “exclusion space” emerges in the mass dimensions to exclude mass and charge deviated from the mass dimensions. The interaction between exclusion space and the particles deviated from the mass dimensions generates the infinite negative “bare mass-charge” to negate the infinite physical mass-charge. Exclusion space establishes renormalization to protect the mass dimensions from physical infinity. Therefore, the mass-charge of the particle with the interaction with exclusion space is the physical source of the bare mass-charge, which is defined conventionally as the mass-charge of the particle without the interaction with virtual particles.

The physical source of exclusion space comes from the empty space of the 10D particle whose mass is dislocated. The 10D particle as the mixed particle consists of internal brane and antibrane. With the CP symmetry, the 10D particle has equal and opposite positive and negative charges for internal brane and antibrane, resulting in the dislocation of energy by the internal annihilation (implosion). The empty space left behind the dislocation is exclusion space, and the dislocated energy is cosmic radiation. Cosmic radiation is forced to travel by exclusion space. The speed of cosmic radiation (light) is dependent of the rate of conversion from ordinary space to exclusion space for the space of cosmic radiation. The 10D particles with CP asymmetry remain as the 10D particles (matter).

The 10D particles as matter absorb exclusion space from cosmic radiation to establish renormalization that allows the immediate fractionalization. The resulting mixture of particles from 4D to 10D has larger size than pure 10D particles, so the fractionalization involves a cosmic expansion. The absorption of exclusion space from cosmic radiation leads to negative pressure for the 10D particles as in the inflation theory [11]. The 10D particles absorb exclusion space exponentially, resulting in exponential inflation. At the beginning of the inflation, inflationary cosmic radiation ( $\phi$ ) has high potential ( $V(\phi)$ ). At the end, all potential is converted into  $\phi$  and exclusion space that induces the immediate fractionalization.

During the inflation, due to the negative pressure from the 10D particles, cosmic radiation is not free to travel. Thus, at the end of the inflation, the particles from 4D to 10D are held together by gravity in the state without expansion and contraction. After the inflation, the absence of the negative pressure allows cosmic radiation to travel freely within the domain of gravity. Free traveling cosmic radiation allows the universe to cool by the non-inflationary decelerating expansion. In summary, the cosmic expansion for the observable universe consists of the inflationary expansion for the immediate fractionalization and the non-inflationary expansion for thermal cooling.

The mixed particles that are not annihilated have asymmetrical charge-parity (CP asymmetry), in such way that the mixed particle has two asymmetrical sets (main and auxiliary) of mass dimensions from the two boundary branes within the mixed particle. The auxiliary set is dependent on the main set, so the mixed particle appears to have only one set of space dimensions. Since there are real and virtual mass dimensions for every particle, there are main real, auxiliary real, main virtual, auxiliary virtual mass dimensions. Thus, for the four-mass-dimensional particle (baryonic matter), there are 4D main real, 4D auxiliary real, 7D main virtual including gravity, and 7D auxiliary virtual mass dimensions. These mass dimensions are for the mixture of leptons and quarks, and form the base for the periodic table of elementary particles [1] as shown later.

The summary of the cosmic evolution by object-space is described in Fig. 7.

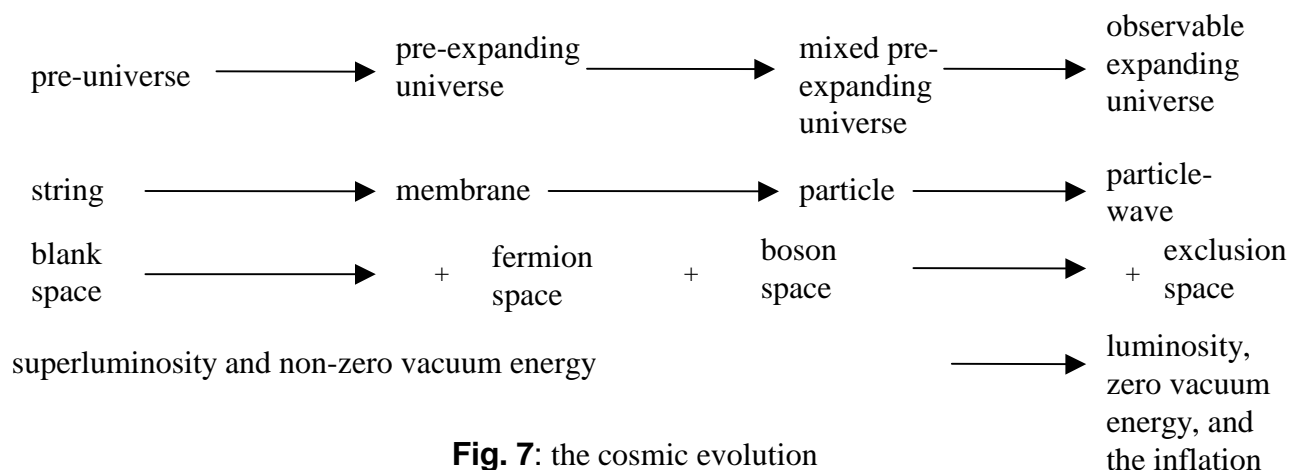


**Fig. 7:** the cosmic evolution

#### 4. *The Space Theory of Quantum Mechanics*

In the space theory of quantum mechanics, quantum mechanics is the interaction of four spaces: blank space, fermion space, boson space, and exclusion space, which overlap among one another after the inflation. The presence of blank space in object is manifested by the creation-annihilation of object. Boson space and fermion space exist complementarily in and around all matters, including both boson and fermion. In one boson space, there are multiple objects, which can also be multiple states in one boson space in one object, so boson space fractionalizes an object into multiple states as wave, while fermion space retains an object as single state as particle. The complementary existence of boson space and fermion space brings about the complementary principle between wave and particle.

Boson space overlaps with exclusion space surrounding a particle. In the overlapping space of boson space and exclusion space, various parts of the overlapping space undergo constant random changes from inclusion to exclusion and from exclusion to inclusion. The rate of change from inclusion to exclusion and from exclusion to inclusion is velocity. The requirement for randomness does not allow constant position and constant velocity

(the rate of change) simultaneously. At an exact position, the variation in velocities is large. At an exact velocity, the variation in positions is large. The variation is uncertainty. This exclusion-inclusion of an object is essentially equivalent to subjective measurement of an object in Copenhagen interpretation of quantum mechanics. Therefore, the source of the uncertainty principle is subjective measurement or the objective exclusion. Consequently, an object has the probability to be anywhere in the form of wavefunction.

During the entanglement of two sets of wavefunction, the original two sets of multiple states from boson space and exclusion space no longer exist. By eliminating exclusion space and boson space, the entangled fermion space with the one state, the entangled state, emerges. This is the collapse of wavefunction. Therefore, any measurement of wavefunction always ends with one state instead of multiple states. The summary is described in Fig. 8.

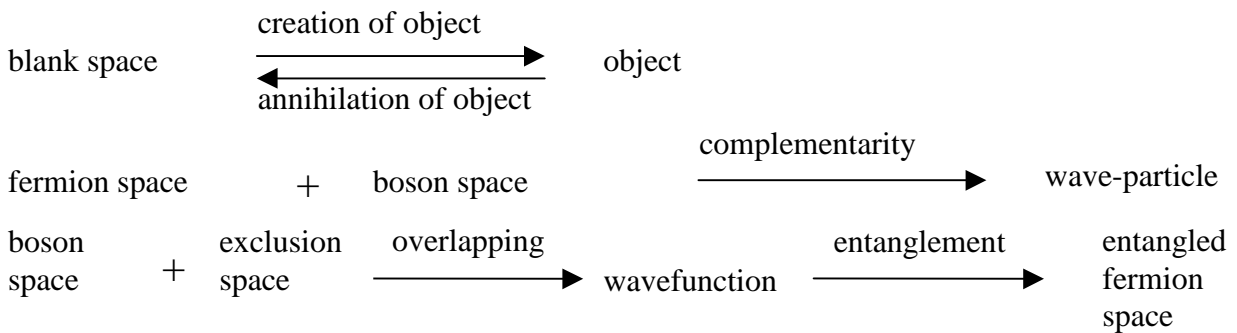


**Fig. 8:** the space theory of quantum mechanics

### 5. *The Cyclic Universe*

The hidden universe and the observable universe are incompatible in dimensionality and in physical laws (with and without exclusion space), so they are completely transparent to each other until they are compatible in dimensionality. This two-universe model appears also in the two-universe (visible and hidden) model in the cyclic ekpyrotic universe model [10].

When the hidden universe fractionalizes into  $4D$  particle compatible with the  $4D$  particle in the observable universe, they form the five dimensional bulk as in the two-sided Randall - Sundrum model [5] as Fig. 9.

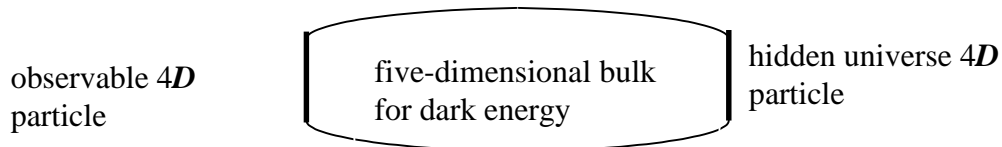


**Fig. 9:** compatible universes and dark energy

The five-dimensional bulk provides space for dark energy (quintessence) [12] as the scalar field from the hidden universe. Dark energy accelerates cosmic expansion in the

observable universe. (With incompatible in physical laws, the two universes are still largely transparent to each other.)

After a certain period in the hidden universe, the  $4D$  particle starts to condense into the  $5D$  particle, inducing contraction in the observable universe. When all of the hidden universe  $4D$  particles is converted into the  $5D$  particles, the incompatible universes return, and dark energy ceases to exist.

Observations of quasars have strongly suggested [13] that the fine structure constant  $\alpha$  at the present is slightly larger than  $\alpha$  in the past. Martinez-Ledesma and Mendoza [14] suggested two fields, the “standard Maxwell’s field and a new scalar field. A generalized Lorentz force is expressed as  $d\mathbf{P}/d\tau = \mathbf{F} \cdot \mathbf{J}_e + M \mathbf{J}_e$ , where  $\tau$  is the proper time and  $\mathbf{P}$  is the 1-form momentum,  $\mathbf{F}$  is the Maxwell 2-form field,  $\mathbf{J}_e$  is total current charge 1-form, and  $M$  is scalar field 0-form. The strength of  $M$  field is tiny to account for the tiny increase  $\Delta\alpha$  of the fine structure constant. ( $\Delta\alpha / \alpha = -0.72 \pm 0.18 \times 10^{-5}$ )  $M$  field is the time dependent dark energy that relates to the time dependent compatibility between the hidden universe and the observable universe.

Dark energy controls the rate of expansion and contraction for the observable universe during the compatible universes period, so eventually both the observable universe and the hidden universe end at the same time. At the end of the contraction, the hidden universe becomes the hidden mixed 9-particle, and the observable universe becomes a cosmic black hole without exclusion space. Without exclusion space, the cosmic black hole is converted back into the observable mixed 9-particle. Therefore, the universe has both sides of the mixed 9-particles as the mixed pre-expanding universe. This mixed pre-expanding universe then starts another cycle of the universe as Fig. 10.

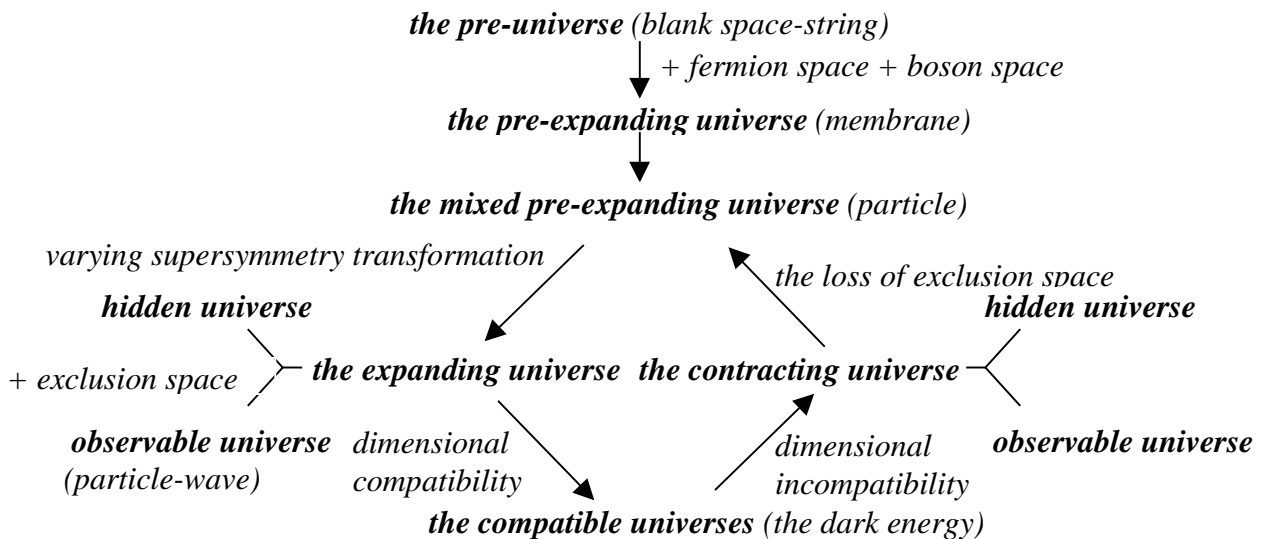


**Fig. 10:** the cyclic universe

## Part 2: The Milky Universe

## 6. *The Formation of Inhomogeneous Structure*

The second major part of the cosmic evolution is the Milky Universe, where the inhomogeneous structures come from the incompatibility between baryonic matter and dark matter.

The observable universe consists of baryonic matter and dark matter. The baryonic matter has the 4-dimensional mass. Dark matter consists of six types of particles with mass dimensions from 5D to 10D. Both dark matter and baryonic matter share the same long-ranged gravity. As shown later, dark matter does not have electromagnetism, so it cannot be seen, but it can be observed by gravity. Such difference in electromagnetism results in the mass dimensional incompatibility between baryonic matter and dark matter. There are seven types of particles from 4D to 10D. Baryonic matter is one of the seven types of particles at equal mass proportions, so the baryonic mass fraction is  $1/7$  (0.14). The universal baryonic mass fraction was found to be 0.13 by the observations of primordial deuterium abundance [15]. The calculated value agrees well with the observed value.

The Inflationary Universe scenario [11] provides possible solutions of the horizon, flatness and formation of structure problems. In the standard inflation theory, quantum fluctuations during the inflation are stretched exponentially so that they can become the seeds for the formation of inhomogeneous structure such as galaxies and galaxy clusters. They also produce anisotropies in CMB (cosmic microwave background). However, without fine-tuning, the calculated amplitude of the density perturbation induced by quantum fluctuations during the inflation is much larger than the observed amplitude in CMB. The small density perturbation is a serious problem in the inflation theory [16].

The universe is supposed to be largely composed of cold dark matter. The density of dark matter is supposed to be the highest (cusp) in the middle of galaxy, but the cusp has not been definitely confirmed by observation [17]. The cusp problem is a serious problem in the theory of dark matter.

In the cosmic evolution, quantum mechanics is fully developed only after the inflation. The inflation does not involve quantum fluctuation, so instead of quantum fluctuations, the incompatibility between ordinary matter and dark matter due to the difference in electromagnetism brings about the formation of inhomogeneous structure. It is analogous to the formation of emulsion (milk) by the incompatibility between two materials such as oil and water. (The incompatibility between oil and water is due to electromagnetic property in terms of polarity.) Such incompatible dark matter (IDM) does not stay permanently in the middle of baryonic matter. Therefore, IDM avoids both the small density perturbation problem and the cusp problem. Incompatible dark matter precludes detecting dark matter on the earth made by baryonic matter.

Cosmic radiation is compatible with both baryonic matter and dark matter through the commonality in exclusion space. The incompatibility between baryonic matter and dark matter increases linearly with decreasing temperature of cosmic radiation whose temperature decreases with increasing size of the universe. Thus, the incompatibility

increases with increasing size of the universe. The whole universe behaves as one unit of emulsion. The mass ratio between baryonic matter and dark matter is 1 to 6. As water domains surround oil droplets (the smaller part) in emulsion, dark matter domains surrounded baryonic droplets (the smaller part). These dark matter domains later became the dark matter halos, and the baryonic droplets became galaxies, clusters, and superclusters.

Incompatible materials separate from each other. The force to maintain the separation is the anti-expansion force to keep one material to expand into the region of other material. The dimensional incompatibility between the baryonic droplet and the dark matter halo is expressed as the interfacial zone between the two different matter domains as Fig. 11.

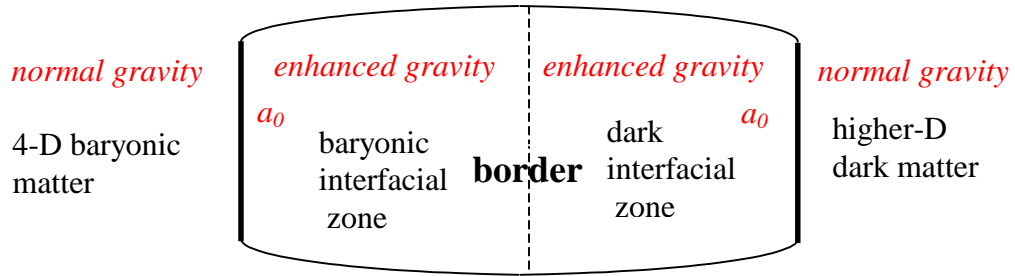


**Fig. 11:** the anti-expansion force in the interfacial zone between baryonic matter and dark matter. The region with the acceleration higher than  $a_0$  has normal gravity, and the interfacial zone with the acceleration lower than  $a_0$  has the enhanced gravity.

The baryon-dark border between baryonic matter and dark matter is in the middle of the interfacial zone. The interfacial zone consists of the dark interfacial zone and the baryonic matter zone for two sides of the baryon-dark border. The force in the interfacial zone is the anti-expansion force as the enhancement of gravity in the interfacial zone away from the baryon-dark border to maintain a clear border. Such enhancement of gravity is same as the enhancement of gravity in the M. Milgrom's [18] Modified Newtonian Dynamics (MOND).

The starting line of the interfacial zone has  $a_0$  as the acceleration. The Newtonian acceleration is  $a_N$ . In the interfacial zone,  $a_N < a_0$ . The effective acceleration  $a_b$  for the baryonic interfacial zone and the  $a_d$  for the dark interfacial zone are as follows.

$$\begin{aligned} a_b &= (a_N a_0)^{1/2} \\ a_d &= (a_N a_0)^{1/2} \end{aligned} \quad (6)$$

$$\text{enhancement of gravity away from the border} \propto (a_0 - a_N)^{1/2} \quad (7)$$

In the equilibrium state,  $a_b$  is symmetrical to  $a_d$ . At a distance,  $r$ , away from the border,

$$\begin{aligned} a_{b,r} &= a_{d,r} \\ (a_0 - a_N)_{b,r}^{1/2} &= (a_0 - a_N)_{d,r}^{1/2} \end{aligned} \quad (8)$$

The enhancement of gravity away from the border in the baryonic interfacial zone results in flat rotation curves as observed in some galaxies [19]. The enhancements of gravity away from the border in both interfacial zones are equal and cancel each other. The net anti-expansion force is zero. This cancellation of the enhancement of gravity is the global cancellation of the deviation (the anti-expansion force) between MOND and Newtonian gravity in a large area that is larger than the interfacial zones. The distance from the center of baryonic mass to the starting line of the interfacial zone increases with increasing  $a_0$ . The size of the universe is directly proportional to  $a_0$ .

As in emulsion, the size of the baryonic droplet grows with increasing incompatibility between dark matter and baryonic matter. As the incompatibility between dark matter and baryonic matter increases with increasing size of the universe, the droplet develops the droplet growth potential as the potential to increase the mass of the droplet. The droplet growth potential converts to the non-zero net anti-expansion force by moving the baryon-dark border outward to absorb free baryonic matter outside and to merge with other droplets. Such movement of the baryon-dark border is derived from the uneven enhancement of gravity in the interfacial zone: high enhancement of gravity away from the border in the dark interfacial zone and low or no enhancement of gravity away from the border in the baryonic interfacial zone.

$$\begin{aligned} a_{b,r} &< a_{d,r} \\ (a_0 - a_N)_{b,r}^{1/2} &< (a_0 - a_N)_{d,r}^{1/2} \end{aligned} \quad (9)$$

In the extreme case,  $a_b = a_N$ , so there is low or no enhancement of gravity in the baryonic interfacial zone as observed as falling rotation curves in bright galaxies [19].

In the case of the trapping of free dark matter inside the baryonic droplet, the incompatibility between dark matter and baryonic matter generates the droplet contraction potential. The potential is to contract the droplet in order to remove the free dark matter inside. The droplet contraction potential converts to the non-zero net anti-expansion force by moving the baryon-dark border inward to expel free dark matter inside. The inward movement involves the uneven enhancement of gravity: low enhancement of gravity in the dark interfacial zone and high enhancement of gravity in the baryonic interfacial zone.

$$\begin{aligned} a_{b,r} &> a_{d,r} \\ (a_0 - a_N)_{b,r}^{1/2} &> (a_0 - a_N)_{d,r}^{1/2} \end{aligned} \quad (10)$$

The high enhancement of gravity away from the border in the baryonic interfacial zone is observed as rising rotation curves in dwarfs and low surface brightness galaxies [19].

In emulsion, oil exists as free oil among water or as oil in oil droplet. Similarly, baryonic matter exists as free baryonic matter among dark matter or as baryonic matter in the baryonic droplet. At the beginning of the expanding universe with high cosmic radiation temperature, baryonic matter and dark matter were completely compatible with each other, and baryonic matter existed entirely as free baryonic matter. As the size of the universe increased, the size of the baryonic droplets increased with the increasing



incompatibility between baryonic matter and dark matter. At the time of recombination (neutralization), the baryonic matter in the small baryonic droplets coexisted with free baryonic matter in the surrounding. With electromagnetic attraction, the baryonic droplet had higher matter density than the surrounding dark matter without electromagnetism and isolated free baryonic matter. The density difference between the baryon matter in the baryonic droplet and the baryonic matter in the surrounding led to anisotropies observed in the CMB.

When the CMB occurred moment before the recombination, because of radiation pressure, the density in the baryonic droplet was much lower than the normal density without radiation pressure. After the decoupling between baryonic matter and radiation at the recombination, the absence of radiation pressure allowed the density of the droplet to return to the normal density quickly.

As the universe expanded, the increasing incompatibility drove increasing amount of free baryonic matter into the baryonic droplets. The growth of the baryonic droplet by the increasing incompatibility from the cosmic expansion coincided with the growth of the baryonic droplet by gravitational instability from the cosmic expansion. The pre-galactic universe consisted of the growing baryonic droplets surrounded by the dark matter halos, which connected among one another in the form of filaments and voids.

## 7. *The Evolution of Galaxies, Clusters, and Superclusters*

When there were many baryonic droplets, the merger among the baryonic droplets became another mechanism to increase the droplet size and mass. In Fig. 12, the baryonic droplets (A and B) merged into one droplet (C). When three or more droplets merged together, dark matter was likely trapped in the merged droplet (D, E, and F in Fig. 12). The droplet with trapped dark matter inside is the heterogeneous baryonic droplet, while the droplet without trapped dark matter inside is the homogeneous baryonic droplet.



**Fig. 12:** the homogeneous baryonic droplets (A, B, and C), and the heterogeneous baryonic droplets (D, E, and F)

For the heterogeneous droplet, the dark matter core is essentially the dark droplet surrounded by the baryonic matter shell. As the dark droplet, the dark matter core has the droplet growth potential proportional to the size of the universe, and has the baryon-dark border moving toward the baryonic matter shell. Thus, two baryon-dark borders in the heterogeneous droplet are the external border between the dark matter halo and the and the dark matter halo and the internal baryon-dark border between the baryonic matter shell and

the dark matter core. The external border moved toward the dark matter halo, while the internal border moved toward the baryonic matter shell. When a section of the internal border and a section of the external border merged, the dark matter from the dark matter core moved to the dark matter halo away from the heterogeneous droplet, and the droplet became homogeneous.

When the temperature dropped to  $\sim 1000^\circ\text{K}$ , some hydrogen atoms in the droplet paired up to create molecular baryonic matter. The most likely place to form such molecular baryonic matter was in the interior part of the droplet. For heterogeneous droplet, molecular baryonic matter formed a molecular layer around the core. Molecular hydrogen cooled the molecular layer by emitting infrared radiation after collision with atomic hydrogen. Eventually, the temperature of the molecular layer dropped to around 200 to  $300^\circ\text{K}$ , reducing the gas pressure and allowing the molecular layer to continue contracting into gravitationally bound dense molecular layer with high viscosity.

Without electromagnetism, the viscosity of dark matter remained low. The viscosity in the dense molecular layer around the core slowed the movement of the internal baryon-dark border toward the baryonic matter shell. On the other hand, the low-viscosity dark matter did not hinder the movement of the external baryon-dark border toward the dark matter halo. The increasing difference in the speeds of movement between the internal and external borders increased the fraction of the heterogeneous baryonic droplets.

Subsequently, the whole baryonic matter shell became the dense molecular layer. The dense baryonic matter shell contracted into gravitationally bound clumps, which prevented the movement of the internal border. The dark matter cores build up the internal pressure from the accumulated droplet growth potential. Eventually, the core with high internal pressure caused the eruption to the droplet. The dark matter rushed out of the droplet within a short time, and the baryonic matter shell collapsed. This eruption is much larger in area and much weaker in intensity than supernova. The “big eruption” of the baryonic droplet brings about the morphologies of galaxies.

If there was very small or no dark matter core as in the homogeneous baryonic droplet, the shape of the resulting galaxy is circular as in the  $E_0$  type elliptical galaxy. If the relative size of the dark matter core was small, the change in the shape of the shell was minor. It is like squeezing out orange juice (dark matter core) through one opening on the orange skin (baryonic matter shell). As the dark matter core moved out, the baryonic matter shell stretched in the opposite direction. The minor change resulted in an elliptical shape as in  $E_1$  to  $E_7$  elliptical galaxies, whose lengths of major axes are proportional to the relative sizes of the dark matter core.

During the collapse of the baryonic matter shell in the big eruption, the collision produced a shock front of high density, which resulted in the formation of many massive first stars. After few million years, such massive first stars became supernovas and black holes. Most of the massive first stars became black holes without contributing to the metal enrichment of the surrounding. The mergers of black holes generated the supermassive black hole as the nucleus of quasar. Such first quasar galaxies that occurred as early as  $z = 6.28$  were observed to have about the same sizes as the Milky Way [20].

The supernova shock wave induced the formation of stars in the exterior part of the droplet. The time difference in the formations of the nucleus and the formation of stars in

the surface was not large, so there are small numbers of observed young stars in elliptical galaxies. This formation of galaxy follows the monolithic collapse model [21], in which baryonic gas in galaxies collapses to form stars within a very short period. Elliptical galaxies continue to grow slowly as the universe expands.

If the size of the dark matter core is medium (D in Fig. 12), it involves a large change on the baryonic matter shell. It is like to release air (the dark matter core) from a balloon (the baryonic matter shell) filled with air. As the dark matter core moved out, the baryonic matter shell moved in the opposite direction.

If there was only one opening as an air balloon with one opening, the dark matter stream from the dark matter core and the baryonic stream from the baryonic matter shell moved in opposite directions. Later, the two streams separated. The dark matter stream merges with the surrounding dark matter. The baryonic stream with high momentum penetrated the surrounding dark matter halo. As the baryonic stream penetrated into the dark matter halo, it met resistance from the anti-expansion force. Eventually, the stream stopped.

The minimization of the interfacial area due to the incomparability between baryonic matter and dark matter transformed the shape of the stream from linear to disk. (The minimization of the interfacial area is shown in the water bead formation on a wax paper.) To transform into disk shape, the stream underwent differential rotation with the increasing angular speeds toward the center. The fast angular speed around the center allowed the winding of the stream around the center. After few rotations, the structure consisted of a bungle was formed by wrapping the stream at the center and the attached spiral arms as spiral galaxy as Fig. 13.

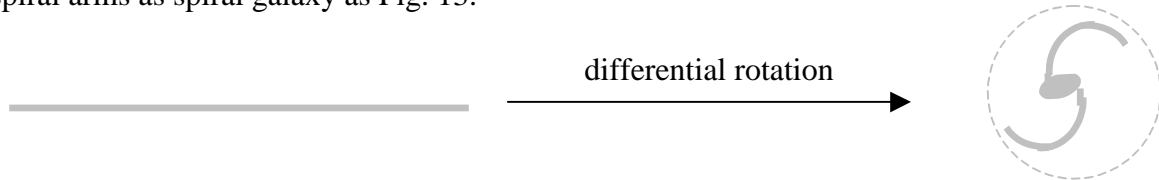


**Fig. 13:** from the linear baryonic stream to normal spiral galaxy with the baryon-dark border (dot line)

During the stream formation, the high-density region derived from the collision during the collapse spread out, so the density of the stream was too low to form stars. As the stream wrapped around at the center, the wrapping of the stream produces the high-density region for the star formation in a steady pace. Thus, the first stars and the black holes at the center in spiral galaxies are smaller than in elliptical galaxies. The stars at the center became black holes and supernovas that induced the star formation in spiral arms. The massive center area decreases the angular speed around the center, greatly retarding the winding of the spiral arms around the center. With this steady pace for the star formation, there are still many young stars in spiral galaxies. When there were more than one baryonic stream in the same general direction, there are more than two spiral arms.

Some streams went through the dark matter halos, and entered into the adjacent baryonic droplets. The adjacent droplet captured a part of the stream, and another part of the stream continued to move to the dark matter halo, and finally settled near the droplet in

the dark matter halo. Dependent on the direction of the entry, the captured part of the stream later became a part of the disk of the host galaxy, star clusters in the halo, or both. The part of the stream that settled near the droplet became the dwarf spheroidal galaxy. Under continuous disruption and absorption of the tidal interaction from the large galaxy nearby, the dwarf spheroidal galaxy does not have well-defined baryonic-dark border, disk, and internal rotation.

When two connected dark matter cores inside far apart from each other (E in Fig. 12) generated two openings in opposite sides of the droplet, the momentum from the two opposite dark matter streams canceled each other nearly completely. The result was the slow moving baryonic droplet. Two opposite baryonic streams formed side by side with the two opposite dark matter streams. When the baryonic stream entered the dark matter halo, the size of the stream decreased due to the anti-expansion force by the dark matter, so there were the thick stream in the baryonic matter shell and the thin stream in the dark matter halo. As the baryonic stream penetrated into the dark matter halo, it met resistance from the anti-expansion force. Eventually, the stream stopped. The result after few differential rotations is the structure with one center, one bar from the thick stream stranding across the center, and arms attached to the bar as bar spiral galaxy as Fig. 14.

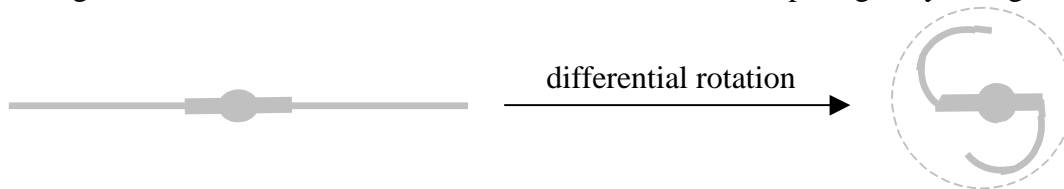


**Fig. 14:** from the barred linear baryonic stream to barred spiral galaxy with the baryon-dark border (dot line)

The result is barred spiral galaxy. As in normal spiral galaxy, the length of the spiral arm depends on the size of the dark matter core. The smallest dark matter core for barred spiral galaxy brings about SBa, and the largest dark matter core brings about SBd. The stars form in the low-density spiral arms much later than in the nucleus, so they are many young stars in the spiral arms.

If the size of the dark matter core was large (F in Fig. 12), the total dark matter mass was nearly large enough or large enough for dark matter to have low droplet growth potential. The escape of the dark matter from the droplet involved little or no eruption, resulting in the gradual migration of large amount of dark matter outward and the gradual migration of small amount of baryonic matter inward. Such opposite migrations are long and continuous processes. The result is irregular galaxy. When enough baryonic matter migrated to the center, and first star formation started. As baryonic matter continues migrating toward the center, the star formation continues in a slow rate up to the present time.

At the end of the big eruption, vast majority of baryonic matter was primordial free baryonic matter resided in dark matter outside of the galaxies from the big eruption. This free baryonic matter constituted the intergalactic medium (IGM). Stellar winds, supernova

winds, and quasars provide heat and heavy elements to the IGM as ionized baryonic atoms. The heat prevented the formation of the baryonic droplet in the IGM.

Galaxies merged into new large galaxies, such as giant elliptical galaxy and cD galaxy ( $z > 1-2$ ). Similar to the transient molecular cloud formation from the ISM (interstellar medium) through turbulence, the tidal debris and turbulence from the mergers generated the numerous transient molecular regions, which located in a broad area [22]. The incompatibility between dark matter and baryonic matter transformed these transient molecular regions into the stable second-generation baryonic droplets surrounded by the dark matter halos. The baryonic droplets had much higher fraction of hydrogen molecules, much lower fraction of dark matter, higher density, and lower temperature, and lower entropy than the surrounding. The baryonic droplets started small with the enormous droplet growth potential. The rapid growth of the baryonic droplets drew large amount of the surrounding IGM inward, generating the IGM flow shown as the cooling flow. The IGM flow induced the galaxy flow. The IGM flow and the galaxy flow moved toward the merged galaxies, resulting in the protocluster ( $z \sim 0.5$ ) with the merged galaxies as the cluster center.

Before the protocluster stage, spirals grew normally and passively by absorbing gas from the IGM as the universe expanded. During the protocluster stage ( $z \sim 0.5$ ), the massive IGM flow injected a large amount of gas into the spirals that joined in the galaxy flow. Most of the injected hot gas passed through the spiral arms and settled in the bungle parts of the spirals. Such surges of gas absorption from the IGM flow resulted in major starbursts ( $z \sim 0.4$ ) [23]. Meanwhile, the nearby baryonic droplets continued to draw the IGM, and the IGM flow and the galaxy flow continued. The results were the formation of high-density region, where the galaxies and the baryonic droplets competed for the IGM as the gas reservoir. Eventually, the maturity of the baryonic droplets caused a decrease in drawing the IGM inward, resulting in the slow IGM flow. Subsequently, the depleted gas reservoir could not support the major starbursts ( $z \sim 0.3$ ). The galaxy harassment and the mergers in this high-density region disrupted the spiral arms of spirals, resulting in S0 galaxies with indistinct spiral arms ( $z \sim 0.1 - 0.25$ ). The transformation process of spirals into S0 galaxies started at the core first, and moved to the outside of the core. Thus, the fraction of spirals decreases with decreasing distance from the cluster center [23].

The static and slow-moving second-generation baryonic droplets turned into dwarf elliptical galaxies and globular clusters. The fast moving second-generation baryonic droplets formed the second-generation baryonic stream, which underwent a differential rotation to minimize the interfacial area between the dark matter and baryonic matter. The result is the formation of blue compact dwarf galaxies (BCD), such as NGC 2915 with very extended spiral arms. Since the star formation is steady and slow, so the stars formed in BCD are new.

The galaxies formed during  $z < 0.1-0.2$  are mostly metal-rich tidal dwarf galaxies (TDG) from tidal tails torn out from interacting galaxies. In some cases, the tidal tail and the baryonic droplet merge to generate the starbursts with higher fraction of molecule than the TDG formed by tidal tail alone [24].

When the interactions among large galaxies were mild, the mild turbulence caused the formation of few molecular regions, which located in narrow area close to the large

galaxies [22]. Such few molecular regions resulted in few baryonic droplets, producing weak IGM flow and galaxy flow. The result is the formation of galaxy group, such as the Local Group, which has fewer dwarf galaxies and lower density environment than cluster.

Clusters merged to generate tidal debris and turbulence, producing the baryonic droplets, the ICM (intra-cluster medium) flow, and the cluster flow. The ICM flow and the cluster flow directed toward the merger areas among clusters and particularly the rich clusters with high numbers of galaxies. The ICM flow is shown as the warm filaments outside of cluster [25]. The dominant structural elements in superclusters are single or multi-branching filaments [26]. The cluster flow is shown by the tendency of the major axes of clusters to point toward neighboring clusters [27]. Eventually at the maximum incompatibility between dark matter and baryonic matter, the observable expanding universe will consist of giant voids and superclusters surrounded by the dark matter halos.

In summary, the whole observable expanding universe is the “Milky Universe” as one unit of emulsion with increasing incompatibility between dark matter and baryonic matter. The five periods of baryonic structure development are the free baryonic matter, the baryonic droplet, the galaxy, cluster, and the supercluster periods as Fig. 15. The first-generation galaxies are elliptical, normal spiral, barred spiral, irregular, and dwarf spheroidal galaxies. The second-generation galaxies are giant ellipticals, cD, evolved S0, dwarf ellipticals, BCD, and TDG. The universe now is in the early part of the supercluster period.

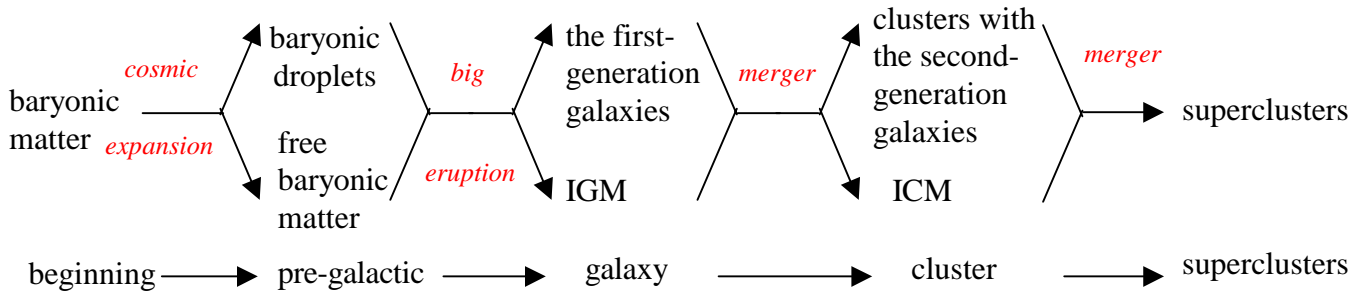


**Fig. 15:** the five levels of baryonic structure in the Milky Universe

### Part 3: The Periodic Table of Elementary Particles

#### 8. *The Force Fields: the Masses of Gauge Bosons*

The third major part of the cosmic evolution is the periodic table of elementary particles for our baryonic matter.

For the four-mass-dimensional particle (baryonic matter), there are 4D main real, 4D auxiliary real, 7D main virtual, and 7D auxiliary virtual mass dimensions. The main and auxiliary real dimensions are for leptons and quarks, respectively. These two sets of

virtual dimensions become the "dimensional orbitals". These hierarchical dimensional orbitals are the force and mass fields, including gravity, as shown in Fig. 16.

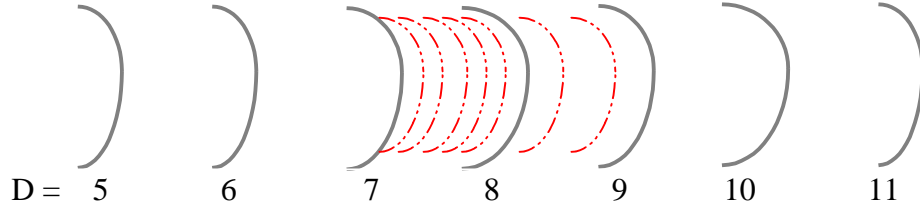


**Fig. 16:** 14 mass-dimensional orbitals in the four-mass dimensional (4D) particle (baryonic matter): 7 main dimensional orbitals (solid line), and 7 auxiliary dimensional orbitals (dot line), D = main dimensional orbital number

As shown in Fig. 16, the auxiliary dimensional orbitals are in the middle of the main dimensional orbitals.

The structure of the 4D particle with dimensional orbitals resembles to the structure of atomic orbital. Consequently, the periodic table of elementary particles is constructed to account of all leptons, quarks, gauge bosons, and hadrons.

For the gauge bosons, the seven main dimensional orbitals are arranged as  $F_5 B_5 F_6 B_6 F_7 B_7 F_8 B_8 F_9 B_9 F_{10} B_{10} F_{11} B_{11}$ , where B and F are boson and fermion in each orbital. The mass dimension in Eq. (5) becomes the main dimensional orbitals with the same equations.

$$M_{D,F} = M_{D,B} \alpha_{D,B}, \quad (11a)$$

$$M_{D-1,B} = M_{D,F} \alpha_{D,F}, \quad (11b)$$

$$M_{D-1,B} = M_{D,B} \alpha_D^2, \quad (11c)$$

where D is the main dimensional orbital number from 6 to 11.  $E_{5,B}$  and  $E_{11,B}$  are the energies for the 5D main dimensional orbital and the 11D main dimensional orbital, respectively. The lowest energy is the Coulombic field,

$$E_{5,B} = \alpha E_{6,F} = \alpha M_e \quad (12)$$

The bosons generated are the main dimensional orbital bosons or  $B_D$ . Using only  $\alpha_e$ , the mass of electron ( $M_e$ ), the mass of  $Z^0$ , and the number (seven) of dimensional orbitals, the masses of  $B_D$  as the gauge boson can be calculated as shown in Table 1.

**Table 1.** The Masses of the main dimensional orbital bosons:  
 $\alpha = \alpha_e$ ,  $D =$  main dimensional orbital number

$B_D$	$M_D$	GeV (calculated)	Gauge boson	Interaction, symmetry	Predecessor
$B_5$	$M_e \alpha$	$3.7 \times 10^{-6}$	A	Electromagnetic, U(1)	pre-charged
$B_6$	$M_6/\alpha$	$7 \times 10^{-2}$	$\pi_{1/2}$	Strong, SU(3) $\longrightarrow$ U(1)	pre-strong
$B_7$	$M_6/\alpha_w^2 \cos \theta_w$	91.177 (given)	$Z_L^0$	weak (left), SU(2) <sub>L</sub>	Fractionalization
$B_8$	$M_7/\alpha^2$	$1.7 \times 10^6$	$X_R$	CP (right) nonconservation, U(1) <sub>R</sub>	CP asymmetry
$B_9$	$M_8/\alpha^2$	$3.2 \times 10^{10}$	$X_L$	CP (left) nonconservation, U(1) <sub>L</sub>	CP asymmetry
$B_{10}$	$M_9/\alpha^2$	$6.0 \times 10^{14}$	$Z_R^0$	weak (right), SU(2) <sub>R</sub>	Fractionalization
$B_{11}$	$M_{10}/\alpha^2$	$1.1 \times 10^{19}$	G	gravity, D particle in D+1 bulk	Pregravity

In Table 1,  $\alpha = \alpha_e$  (the fine structure constant for electromagnetic field), and  $\alpha_w$  is not same as  $\alpha$  of the rest, because as shown later, there is a mixing between  $B_5$  and  $B_7$  as the symmetry mixing between U(1) and SU(2) in the standard theory of the electroweak interaction, and  $\sin \theta_w$  is not equal to 1. As shown later,  $B_5$ ,  $B_6$ ,  $B_7$ ,  $B_8$ ,  $B_9$ , and  $B_{10}$  are A (massless photon),  $\pi_{1/2}$ ,  $Z_L^0$ ,  $X_R$ ,  $X_L$ , and  $Z_R^0$ , respectively, responsible for the electromagnetic field, the strong interaction, the weak (left handed) interaction, the CP (right handed) nonconservation, the CP (left handed) nonconservation, and the P (right handed) nonconservation, respectively. The calculated value for  $\theta_w$  is  $29.69^0$  in good agreement with  $28.7^0$  for the observed value of  $\theta_w$  [28]. The calculated energy for  $B_{11}$  is  $1.1 \times 10^{19}$  GeV in good agreement with the Planck mass,  $1.2 \times 10^{19}$  GeV.

There are dualities between dimensional orbitals and the cosmic evolution. The pre-charged force, the pre-strong force, the fractionalization during the superluminal inflation, the CP asymmetry to generate matter during the inflation, and the pregravity are the predecessors of electromagnetic force, the strong force, the weak interaction, the CP nonconservation, and gravity, respectively. These forces are manifested in the main dimensional orbitals with various space-time symmetries and gauge symmetries. The strengths of these forces are different than their predecessors, and are arranged according to the dimensional orbitals. Each of the forces will be discussed as follows.

The pre-charged force is the predecessor of electromagnetism as the long-ranged force with the absorption-emission of massless particles with U(1) symmetry. Being the main dimensional orbital with the lowest mass,  $B_5$  is the utmost orbital, so as the utmost pre-charged force in the  $10D \times 1D$  Kaluza-Klein structure, electromagnetism is  $B_5$ .

There is duality between the collapse of the pre-expanding universe and electromagnetism. The attraction between the 9-brane and the 9-antibrane is manifested as electric force. As the collapse of the pre-expanding universe begins, and the 9-brane and the 9-antibrane start to move, the attractive force and the repulsive force cause an inversion that turns the 9-brane and the 9-antibrane inside, and turns pregravity and the anti-pregravity outside. In the observable universe, there is no repulsive force between pregravity and the anti-pregravity, so the force for the inversion is manifested as the force



for the rotation, which is magnetic force, perpendicular to the direction of moving charging particles.

Only the 4D particle (baryonic matter) has the  $B_5$ , so without  $B_5$ , dark matter consists of permanently neutral higher dimensional particles. It cannot emit light, cannot form atoms, and exists as neutral gas.

The short-ranged pre-strong force is the predecessor of the short-ranged strong force for quarks with the absorption-emission of massless particles through non-zero energy medium, pions. The pre-strong force is next to the pre-charged force, so the strong force for quarks is  $B_6$  next to  $B_5$  for electromagnetism. There is duality between  $B_6$  and the hiding of quark as the auxiliary particle in the 4D particle. Lepton is the main particle.

The hypercharges for both  $e^+$  and  $\nu$  are 1, while for both u and d quarks, they are 1/3. The electric charges for  $e^+$  and  $\nu$  are 1 and 0, respectively, while for u and d quarks, they are 2/3 and -1/3, respectively. The hiding of quark is achieved by the strong interaction for quark. The hiding is generated by "leptonization" [29], which means quarks have to behave like leptons in the main dimensional orbitals. Leptons have integer electric charges and hypercharges, while quarks have fractional electric charges and hypercharges. The leptonization is to make quarks behave like leptons in terms of "apparent" integer electric charges and hypercharges. There are two parts for this strong interaction: the first part is for the charge, and the second part is for the hypercharge. The first part of the strong interaction allows the combination of a quark and an antiquark in a particle, so there is no fractional electric charge. It involves the conversion of  $\pi_{1/2}$  boson in  $B_6$  into the electrically chargeless meson field by combining two  $\pi_{1/2}$ , analogous to the combination of  $e^+$  and  $e^-$  fields, so the meson field becomes chargeless. (The mass of  $\pi$ , 135 MeV, is twice of the mass of a half-pion boson, 70 MeV, minus the binding energy.  $\pi_{1/2}$  becomes pseudoscalar up or down quark in pion.) In the meson field, no fractional charge of quark can appear. The second part of the strong interaction is to combine three quarks in a particle, so there is no fractional hypercharge. It involves the conversion of  $B_5$  ( $\pi_{1/2}$ ) into the gluon field with three colors. The number of colors (three) in the gluon field is equal to the ratio between the lepton hypercharge and quark hypercharge. There are three  $\pi_{1/2}$  in the gluon field, and at any time, only one of the three colors appears in a quark. Quarks appear only when there is a combination of all three colors or color-anticolor. In the gluon field, no fractional hypercharge of quarks can appear. By combining both of the meson field and the gluon field, the strong interaction is the three-color gluon field based on the chargeless vector meson field from the combination of two  $\pi_{1/2}$ 's. The total number of  $\pi_{1/2}$  is 6, so the fine structure constant,  $\alpha_s$ , for the strong force is

$$\alpha_s = 6 \alpha e^1 = 0.119 \quad (13)$$

which is in a good agreement with the observed value, 0.124 [30]. Without colors, leptons do not have the strong force.

The fractionalization of the particles during the inflation is the predecessor of the weak interaction for the changes of the flavors (masses) of particles. The two fractionalizations in the opposite sides (hidden and observable) of the expanding universe

are chiral, so the weak interaction is chiral. The fractionalization involves the uneven supersymmetry transformation of a particle into a lower dimensional and lower mass particle. In the weak interaction, gauge symmetry for the absorption and the emission of massive particle replaces the supersymmetry transformation that is no longer possible. The method for such replacement is for the weak interaction to take part in the formation of electric charge, which involves the absorption and the emission of massless particle. It is the U(1) x SU(2) mixing to form electric charge. U(1) is the non-fractionalization from the pre-electromagnetism, so assign hypercharge of 1 to both pre- $e^+$  and pre- $\nu$ , respectively. In SU(2), pre- $e^+$  and pre- $\nu$  are before and after the fractionalization, respectively, so assign isospin 1/2 and -1/2 to pre- $e^+$  and pre- $\nu$ , respectively. The mixing of U(1) and SU(2) leads to electric charge = hypercharge/2 + isospin. The electric charges of  $e^+$  and  $\nu$  are equal to 1 and 0, respectively.

$B_7$  carries the charge for the gauge symmetry for the weak interaction within the family of leptons or quarks at different dimensional orbitals. There is the mixing between  $B_5$  and  $B_7$ , corresponding to the U(1) x SU(2) mixing. The absolute or nearly absolute chiral symmetry (permanent chirality) generates massless or nearly massless neutrinos.

The CP asymmetry to generate matter during the inflation is the predecessor of the CP nonconservation that is  $B_9$  for CP (left) with U(1) symmetry. For the reason of symmetry, P and CP nonconservations are in pairs of the right and the left.  $B_7$ ,  $B_8$ ,  $B_9$ , and  $B_{10}$  carry P (left), CP (right), CP (left), and P (right) nonconservation, respectively. However, only P (left) at  $B_7$  and CP (left) at  $B_9$  relate to the fractionalization and the CP asymmetry to generate matter, respectively, in the observable universe.

The dimensional boson,  $B_8$ , is a CP (right). The ratio of the force constants between the CP-invariant  $W_L$  in  $B_8$  and the CP-violating  $X_R$  in  $B_8$  is

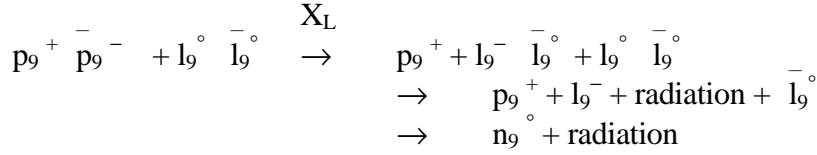
$$\begin{aligned} \frac{G_8}{G_7} &= \frac{\alpha E_7^2 \cos^2 \Theta_w}{\alpha_w E_8^2} \\ &= 5.3 \times 10^{-10} \quad , \end{aligned} \tag{14}$$

which is in the same order as the ratio of the force constants between the CP-invariant weak interaction and the CP-violating interaction with  $|\Delta S| = 2$ . The  $B_8$  does not generate matter.

The dimensional boson,  $B_9$  ( $X_L$ ), has the CP-violating U(1)<sub>L</sub> symmetry.  $B_9$  generates matter. As shown in Fig. 17, the lepton ( $l_9$ ) and the quark ( $q_9$ ) are outside of the three families for leptons and quarks, so baryons in dimension nine do not have to have the baryon number conservation. The baryon that does not conserve baryon number has the baryon number of zero. The combination of the CP-nonconservation and the baryon number of zero leads to the baryon,  $\bar{p}_9^-$ , with the baryon number of zero and the baryon,  $p_9^+$ , with the baryon number of 1. The decay of the baryon  $\bar{p}_9^-$  with zero baryon number into the leptons, whose sum of lepton numbers is zero, is as follows.

$$\bar{p}_9^- \rightarrow l_9^- \bar{l}_9^0$$

The combination this  $p_9^-$  and  $p_9^+$  as well as leptons  $l_9^+$   $l_9^-$  and gauge boson  $X_L$  results in



Consequently, excess baryons,  $n_9^+$ , are generated in the dimension nine. These excess baryons,  $n_9^+$ , become the predecessors of excess neutrons in the low energy level.

The ratio of force constants between  $X_R$  with CP conservation and  $X_L$  with CP-nonconservation is

$$\begin{aligned}
 \frac{G_9}{G_8} &= \frac{\alpha E_8^2}{\alpha E_9^2} \\
 &= 2.8 \times 10^{-9} \quad ,
 \end{aligned} \tag{15}$$

which is the ratio of the numbers between matter (dark and baryonic) and photons in the universe. The mass of baryonic matter is 1/7 of the total mass of matter, and the number of baryonic matter is approximately 1/3 to 1/4 of the total number of matter. Hence, the ratio of the numbers between baryonic matter and photons is about 7 to  $9 \times 10^{-10}$ , which is close to the ratio (around  $5 \times 10^{-10}$ ) obtained by the big bang nucleosynthesis.

Gravity, the individualized pregravity, continues to have the same long-ranged force with the Planck-infinite dimension as pregravity. Therefore, gravity continues to be  $B_{11}$  with the Planck mass. The summary of all forces and their predecessors is in Table 1.

## 9. *The Periodic Table of Elementary Particles: the Masses of Leptons and Quarks*

The two sets of seven dimensional orbitals result in 14 dimensional orbitals (Fig. 17) for gauge bosons, leptons, and quarks. The periodic table for elementary particles is shown in Table 2.

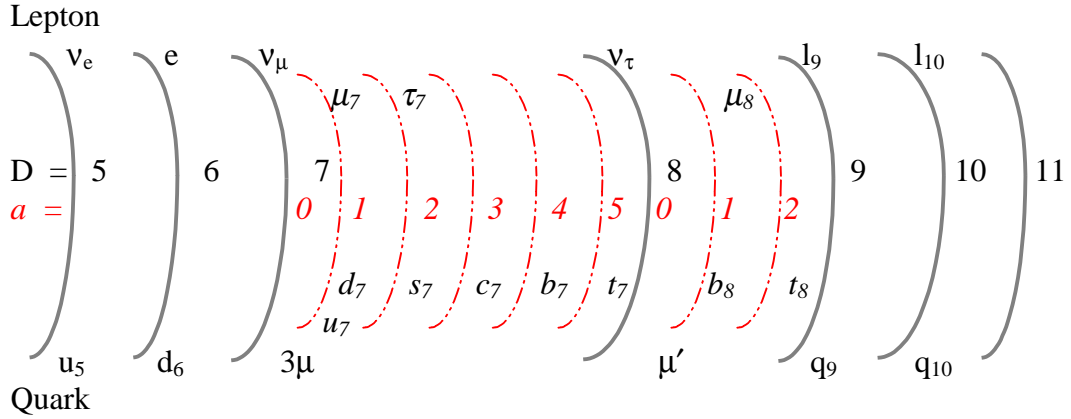


**Fig. 17:** leptons and quarks in the dimensional orbits  
D = main dimensional number, a = auxiliary dimensional number

**Table 2.** The Periodic Table of elementary particles

D = main dimensional orbital number, a = auxiliary dimensional orbital number

D	a = 0	1	2	a = 0	1	2	3	4	5	
	<u>Lepton</u>			<u>Quark</u>					<u>Boson</u>	
5	$l_5 = \nu_e$			$q_5 = u_5 = 3\nu_e$					$B_5 = A$	
6	$l_6 = e$			$q_6 = d_6 = 3e$					$B_6 = \pi_{1/2}$	
7	$l_7 = \nu_\mu$	$\mu_7$	$\tau_7$	$q_7 = 3\mu$	$u_7/d_7$	$s_7$	$c_7$	$b_7$	$t_7$	$B_7 = Z_L^0$
8	$l_8 = \nu_\tau$	$\mu_8$		$q_8 = \mu'$	$b_8$	$t_8$				$B_8 = X_R$
9	$l_9$			$q_9$						$B_9 = X_L$
10	$f_{10}$									$B_{10} = Z_R^0$
11	$f_{11}$									$B_{11} = G$

D is the dimensional orbital number for the seven main dimensional orbitals. The auxiliary dimensional orbital number, a, is for the seven extra auxiliary dimensional orbitals. All gauge bosons, leptons, and quarks are located on the seven main dimensional orbits and seven auxiliary orbits.  $\nu_e$ ,  $e$ ,  $\nu_\mu$ , and  $\nu_\tau$  are main dimensional fermions for main dimension 5, 6, 7, and 8, respectively. All neutrinos have zero mass because of chiral symmetry (permanent chirality).

The dimensional fermions for D = 5 and 6 are neutrino ( $l_5$ ) and electron ( $l_6$ ), respectively. To generate a quark whose mass is higher than the lepton is to add the lepton to the boson from the combined lepton-antilepton, so the mass of the quark is three times of the mass of the corresponding lepton in the same main dimension. The equation for the quark mass is

$$M_{q_D} = 3M_{l_D} \quad (16)$$

A heavy lepton ( $\mu$  or  $\tau$ ) is the combination of the dimensional leptons and the auxiliary dimensional leptons. In the same way, a heavy quark is the combination of the dimensional quarks from Eq.(16) and the auxiliary quarks. The mass of the auxiliary dimensional fermion (AF for both heavy lepton and heavy quark) is generated from the corresponding main dimensional boson as follows.

$$M_{AF_{D,a}} = \frac{M_{B_{D-1,0}}}{\alpha_a} \sum_{a=0}^a a^4, \quad (17)$$

where  $\alpha_a$  = auxiliary dimensional fine structure constant, and  $a$  = auxiliary dimension number = 0 or integer. The first term,  $\frac{M_{B_{D-1,0}}}{\alpha_a}$ , of the mass formula (Eq. (17)) for the auxiliary dimensional fermions is derived from the mass equation, Eq. (11), for the dimensional fermions and bosons. The second term,  $\sum_{a=0}^a a^4$ , of the mass formula is for Bohr-Sommerfeld quantization for a charge - dipole interaction in a circular orbit as described by A. O. Barut [2].  $1/\alpha_a$  is  $3/2$ . The coefficient,  $3/2$ , is to convert the main dimensional boson mass to the mass of the auxiliary dimensional fermion in the higher dimension by adding the boson mass to its fermion mass which is one-half of the boson mass. The formula for the mass of auxiliary dimensional fermions (AF) becomes

$$\begin{aligned} M_{AF_{D,a}} &= \frac{M_{B_{D-1,0}}}{\alpha_a} \sum_{a=0}^a a^4 \\ &= \frac{3}{2} M_{B_{D-1,0}} \sum_{a=0}^a a^4 \\ &= \frac{3}{2} M_{F_{D,0}} \alpha_D \sum_{a=0}^a a^4 \end{aligned} \quad (18)$$

When the mass of this auxiliary dimensional fermion is added to the sum of masses from the corresponding main dimensional fermions (zero auxiliary dimension number) with the same electric charge and the same main dimension, the fermion mass formula for heavy leptons and quarks is derived as follows.

$$\begin{aligned} M_{F_{D,a}} &= \sum M_{F_{D,0}} + M_{AF_{D,a}} \\ &= \sum M_{F_{D,0}} + \frac{3}{2} M_{B_{D-1,0}} \sum_{a=0}^a a^4 \\ &= \sum M_{F_{D,0}} + \frac{3}{2} M_{F_{D,0}} \alpha_D \sum_{a=0}^a a^4 \end{aligned} \quad (19)$$

Each fermion can be defined by main dimensional numbers (D's) and auxiliary dimensional numbers (a's). Heavy leptons and quarks consist of one or more D's and a's. The compositions and calculated masses of leptons and quarks are listed in Table 3.

**Table 3.** The Compositions and the Constituent Masses of Leptons and Quarks  
D = main dimensional orbital number and a = auxiliary dimensional orbital number

	$D_a$	Composition	Calc. Mass
<u>Leptons</u>	<u><math>D_a</math> for leptons</u>		
$\nu_e$	$5_0$	$\nu_e$	0
E	$6_0$	e	0.51 MeV (given)
$\nu_\mu$	$7_0$	$\nu_\mu$	0
$\nu_\tau$	$8_0$	$\nu_\tau$	0
$\mu$	$6_0 + 7_0 + 7_1$	$e + \nu_\mu + \mu_7$	105.6 MeV
$\tau$	$6_0 + 7_0 + 7_2$	$e + \nu_\mu + \tau_7$	1786 MeV
<u>Quarks</u>	<u><math>D_a</math> for quarks</u>		
u	$5_0 + 7_0 + 7_1$	$u_5 + q_7 + u_7$	330.8 MeV
d	$6_0 + 7_0 + 7_1$	$d_6 + q_7 + d_7$	332.3 MeV
s	$6_0 + 7_0 + 7_2$	$d_6 + q_7 + s_7$	558 MeV
c	$5_0 + 7_0 + 7_3$	$u_5 + q_7 + c_7$	1701 MeV
b	$6_0 + 7_0 + 7_4$	$d_6 + q_7 + b_7$	5318 MeV
t	$5_0 + 7_0 + 7_5 + 8_0 + 8_2$	$u_5 + q_7 + t_7 + q_8 + t_8$	176.5 GeV

The lepton for main dimension five is  $\nu_e$ , and the quark for the same main dimension is  $u_5$ , whose mass is equal to  $3 M\nu_e$  from Eq. (16). The lepton for the main dimension six is e, and the quark for this main dimension is  $d_6$ .  $u_5$  and  $d_6$  represent the “light quarks” or “current quarks” which have low masses. The main dimensional lepton for the dimensions seven is  $\nu_\mu$ . All  $\nu$ 's become massless by the chiral symmetry to preserve chirality. The auxiliary dimensional leptons (Al) in the main dimension seven are  $\mu_7$  and  $\tau_7$  whose masses can be calculated by Eq. (20) derived from Eq. (18).

$$\begin{aligned}
 M_{Al7,a} &= \frac{3}{2} M_{B_{6,0}} \sum_{a=0}^a a^4 \\
 &= \frac{3}{2} M_{\pi_{1/2}} \sum_{a=0}^a a^4 \quad ,
 \end{aligned}
 \tag{20}$$

where  $a = 1, 2$  for  $\mu_7$  and  $\tau_7$ , respectively.

For heavy quarks,  $q_7$  (the main dimensional fermion,  $F_7$ , for quarks in the main dimension seven) is  $3\mu$  instead of massless  $3v$  as in Eq. (16). According to the mass formula, Eq. (18), of the auxiliary fermion, the mass formula for the auxiliary quarks,  $Aq_{7,a}$ , is as follows.

$$\begin{aligned} M_{Aq_{7,a}} &= \frac{3}{2} M_{q_7} \alpha_7 \sum_{a=0}^a a^4 \\ &= \frac{3}{2} (3 M_\mu) \alpha_w \sum_{a=0}^a a^4 \quad , \end{aligned} \tag{21}$$

where  $\alpha_7 = \alpha_w$ , and  $a = 1, 2, 3, 4,$  and  $5$  for  $u_7/d_7, s_7, c_7, b_7,$  and  $t_7,$  respectively.

The main dimensional lepton for the main dimension eight is  $\nu_\tau$ , whose mass is zero to preserve chirality. The heavy lepton for the main dimensional eight is  $\mu'$  as the sum of  $e, \mu,$  and  $\mu_8$  (auxiliary dimensional lepton). Because there are only three families for leptons,  $\mu'$  is the extra lepton, which is "hidden".  $\mu'$  can appear only as  $\mu + \text{photon}$ . The pairing of  $\mu + \mu$  from the hidden  $\mu'$  and regular  $\mu$  may account for the occurrence of same sign dilepton in the high energy level [31]. For the main dimension eight,  $q_8$  (the  $F_8$  for quarks) is  $\mu'$  instead of  $3\mu'$ , because the hiding of  $\mu'$  allows  $q_8$  to be  $\mu'$ . The hiding of  $\mu'$  for leptons is balanced by the hiding of  $b_8$  for quarks. The calculated masses are in good agreement with the observed constituent masses of leptons and quarks [32] [33]. The observed mass of the top quark is  $174.3 \pm 5.1$  GeV [33] in a good agreement with the calculated value, 176.5 GeV. The masses of leptons, quarks, gauge bosons, and hadrons are calculated with only four known constants: the number of spatial dimensions, the mass of electron, the mass of  $Z^0$ , and  $\alpha_e$ .

## 10. *The Masses of Hadrons*

As molecules are the composites of atoms, hadrons are the composites of elementary particles. Hadron can be represented by the nonrelativistic constituent quark model where the mass of a hadron is the sum of the masses of quarks plus a relatively small binding energy.  $\pi_{1/2}$  (u or d pseudoscalar quark), u, d, s, c, b, and t quarks mentioned above are nonrelativistic constituent quarks. On the other hand, except proton and neutron, all hadrons are unstable, and decay eventually into low-mass quarks and leptons. Therefore, hadrons are the composition of both quarks and the "transitional blocks" which are the smallest units in leptons and quarks, common for all leptons and quarks. Such transitional blocks cannot be isolated. The precise masses of hadrons are derived from the compositions of the transitional blocks within the compositions of constituent quarks. The masses of hadrons are calculated by a dual formula consisting of the quark formula and the block formula. The quark formula consists of for all nonrelativistic constituent quarks ( $\pi_{1/2}, u, d, s, c,$  and  $b$ ), and the block formula consists of the lowest- mass quark ( $\pi_{1/2}$  and  $u$ ) and lepton ( $e$ ). The calculation of the masses of hadrons requires both formulas. The quark formula sets the initial mass for a hadron. This initial mass is matched by the mass resulted from the combination of various

blocks in the block formula. The mass of a hadron is the mass of the block formula plus the binding energy (negative energy).

$$M_{\text{quark formula}} \approx M_{\text{block formula}}$$

$$M_{\text{hadron}} = M_{\text{block formula}} + \text{binding energy} \quad (22)$$

This dual representation of hadrons by the quark formula and the basic quark formula is seen in the treatment of nucleons [34] as a mixture of the quark model and the vector meson dominance model which can be represented by  $\pi_{1/2}$  and u.

The quark formula consists of the vector quarks (u, d, s, c, and b) and pseudoscalar quark,  $\pi_{1/2}$  (70.03 MeV), which is  $B_6$  (dimension boson in the dimension six).  $\pi_{1/2}$  is designated as “m” for basic mass block. The strong interaction converts  $B_6$  ( $\pi_{1/2}$ ) into pseudoscalar u and d quark in pseudoscalar  $\pi$  meson. The combination of the pseudoscalar quark ( $\pi_{1/2}$ ) and vector quarks (q) results in hybrid quarks (q') whose mass is the average mass of pseudoscalar quark and vector quark.

$$M_{q'} = 1/2 (M_q + M_m) \quad (23)$$

Hybrid quarks include u', d', and s' whose masses are 200.398, 201.164, and 314.148 MeV, respectively. For baryons other than n and p, the quark formula is the combination of vector quarks, hybrid quarks (u' and d'), and pseudoscalar quark ( $\pi_{1/2}$ ). For example,  $\Lambda^\circ$  (uds) is u'd's  $m_3$ , where  $m_3$  denotes 3  $\pi_{1/2}$ . For pseudoscalar mesons (J = 0), the quark formula is the combination of m and q' (u', d' and s') or m alone. For vector mesons (J > 0), the quark formula is the combination of vector quarks (u, d, s, c, and b) and m. For examples,  $\pi^\circ$  is  $m_2$ ,  $\eta$  (1295, J=0) is u'u'd'd'  $m_8$ , and  $K_1$  (1400, J=1) is ds  $m_8$ . The compositions of hadrons from the particles of the quark formula are listed in Table 4.

**Table 4.** Particles for the quark formula

	m	u', d'	s'	u, d	s	c, b
mass (MeV) (from Tables 1 and 3 and Eq. (23))	70.025	200.40, 201.16	314.15	330.8, 332.3	558	1701, 5318
n and p				√		
Baryons other than n and p	√	√			√	√
Mesons (J = 0) except $c \bar{c}$ and $b \bar{b}$	√	√	√			√
Mesons (J > 0) and $c \bar{c}$ and $b \bar{b}$	√			√	√	√

The block formula comes from M. H. MacGregor's constant quark model [3], whose calculated masses and the predicted properties of hadrons are in very good agreement with observations. In the constituent quark model, the mass building blocks



are the "spinor" (S with mass 330.4 MeV) and the mass quantum (mass = 70MeV). For the block formula, S is U, the quark with the lowest mass (330.77 MeV), and the basic quantum is  $\pi_{1/2}$  (mass = 70.025 MeV). Six m ( $m_6$ ) appears often as a block as demonstrated in the constituent quark model, so  $m_6$  is represented by X. For examples, in the block formula, neutron is UUU or  $U_3$ , and  $f_0$  (980) is  $m_{14}$  or  $m_2X_2$ .

In additional to U and m, the blocks in the block formula includes P (positive charge) and N (neutral charge) with the masses of proton and neutron. As in the constituent quark model, the mass associated with positive or negative charge is the electromagnetic mass, 4.599 MeV, which is nine times the mass of electron. This mass (nine times the mass of electron) is derived from the baryon-like electron that represents three quarks in a baryon and three electrons in  $d_6$  quark as in Table 2. This electromagnetic mass is the baryonic electromagnetic mass. This electromagnetic mass is observed in the mass difference between  $\pi^\circ$  ( $m_2$ ) and  $\pi^+$  ( $m_{2+}$ ) where + denotes positive charge. The calculated mass different is one electromagnetic mass, 4.599 MeV, in good agreement with the observed mass difference, 4.594 MeV, between  $\pi^\circ$  and  $\pi^+$ . For  $\tau$ , the difference between the calculated mass (1786 MeV) by the Barut lepton mass formula and the observed mass ( $\approx 1777$  MeV) is about 9 MeV, which is twice of the baryonic electromagnetic mass, caused by the contribution of  $\tau$  to the baryon formation. (The values for observed masses are taken from "Particle Physics Summary "[33].) The particles in the block formula are listed in Table 5.

**Table 5.** Blocks in the block formula

Blocks	m	X	U	N	P	Electromagnetic mass
Origins in quarks	$\pi_{1/2}$	$6 \pi_{1/2}$	u quark	n	p	9 e
Mass (MeV)	70.0254	420.2 or 405	330.77	939.565	938.272	4.599

Hadrons are the composites of quarks as molecules composing of atoms. As atoms are bounded together by chemical bonds, hadrons are bounded by "hadronic bonds," connecting the blocks in the block formula. These hadronic bonds are similar to the hadronic bonds in the constituent quark model.

The hadronic bonds are the overlappings of the auxiliary dimensional orbitals. From Eq (18), the energy for the auxiliary orbital for U (u quark) is

$$\begin{aligned} E_a &= (3/2) (3 M_\mu) \alpha_w \\ &= 14.122 \text{ MeV} \end{aligned} \quad (24)$$

The auxiliary orbital is a charge - dipole interaction in a circular orbit as described by A. O. Barut [2], so a fermion for the circular orbit and an electron for the charge are embedded in this hadronic bond. The fermion for the circular orbit is the supersymmetry fermion for the auxiliary dimensional orbit according to Eq (11a).

$$M_f = E_a \alpha_w \quad (25)$$

The binding energy (negative energy) for the bond (U , U) between two U's is twice of 14.122 MeV minus the masses of the supersymmetry fermion and electron.

$$\begin{aligned} E_{U-U} &= -2 (E_a - M_f - M_e) \\ &= -26.384 \text{ MeV} \end{aligned} \quad (26)$$

It is similar to the binding energy (-26 MeV) in the constituent quark model. An example of U , U bond is in neutron (U – U – U) which has two U – U bonds. The mass of neutron can be calculated as follows.

$$\begin{aligned} M_n &= 3M_U + 2E_{U-U} \\ &= 939.54 \text{ MeV}, \end{aligned} \quad (27)$$

which is in excellent agreement with the observed mass, 939.57 MeV. The mass of proton is the mass of neutron minus the mass difference (three times of electron mass =  $M_{3e}$ ) between u and d quark as shown in Table 2. Proton is represented as U – U – (U -3e). The calculation of the mass of proton is as follows.

$$\begin{aligned} E_a \text{ for (U-3e)} &= (3/2) (3 (M_\mu - M_{3e})) \alpha_w \\ M_f &= E_a \alpha_w \\ M_p &= 2 M_U + M_{(U-3e)} + E_{U,U} + E_{U,(U-3e)} \\ &= 938.21 \text{ MeV} \end{aligned} \quad (28)$$

The calculated mass is in a good agreement with the observed mass, 938.27 MeV.

The binding energy for m – m ( $\pi_{1/2} - \pi_{1/2}$ ) bond can be derived in the same way as Eqs (24), (25), and (26).

$$\begin{aligned} E_a &= (3/2) M_m \alpha_w \\ M_f &= E_a \alpha_w \\ E_{m-m} &= -2 (E_a - M_f - M_e) \\ &= -5.0387 \text{ MeV} \end{aligned} \quad (29)$$

It is similar to the binding energy (-5 MeV) in the constituent quark model. An example for the binding energy of m - m bond is in  $\pi^\circ$ . The mass of  $\pi^\circ$  can be calculated as follows.

$$\begin{aligned} M_{\pi^\circ} &= 2 M_m + E_{m-m} \\ &= 135.01 \text{ MeV}. \end{aligned} \quad (30)$$

The calculated mass of  $\pi^\circ$  is in excellent agreement with the observed value, 134.98 MeV. There is one m - m bond per pair of m 's, so there are two m - m bonds for 4 m 's, and three m - m bonds for 6 m 's.

Another bond is N – m or P – m, the bond between neutron or proton and m. Since N is UUU, N – m bond is derived from U – m. The binding energy of U – m is the average between U–U and m - m.

$$E_{U-m} = 1/2 (E_{U-U} + E_{m-m}) \quad (31)$$

An additional dipole ( $e^+e^-$ ) is needed to connect U – m to neutron.

$$\begin{aligned} E_{N-m} &= E_{U-m} + 2 M_e \\ &= -14.689 \text{ MeV}. \end{aligned} \quad (32)$$

It is similar to the binding energy (-5 MeV) in the constituent quark model. An example for the binding energy of m - m bond is in  $\pi^0$ . The mass of  $\pi^0$  can be calculated as follows.

$$\begin{aligned} M_{\pi^0} &= 2 M_m + E_{m-m} \\ &= 135.01 \text{ MeV}. \end{aligned} \quad (30)$$

The calculated mass of  $\pi^0$  is in excellent agreement with the observed value, 134.98 MeV. There is one m - m bond per pair of m 's, so there are two m - m bonds for 4 m 's, and three m - m bonds for 6 m 's.

Another bond is N – m or P – m, the bond between neutron or proton and m. Since N is UUU, N – m bond is derived from U – m. The binding energy of U – m is the average between U–U and m - m.

$$E_{U-m} = 1/2 (E_{U-U} + E_{m-m}) \quad (31)$$

An additional dipole ( $e^+e^-$ ) is needed to connect U – m to neutron.

$$\begin{aligned} E_{N-m} &= E_{U-m} + 2 M_e \\ &= -14.689 \text{ MeV}. \end{aligned} \quad (32)$$

It is similar to -15 MeV in the constituent quark model. An example for P–m is  $\Sigma^+$  which is represented by  $Pm_4$  whose structure is  $m_2 -P-m_2$ . The 4 m 's are connected to P with two P–m bonds. The mass of  $\Sigma^+$  is as follows.

$$\begin{aligned} M_{\Sigma^+} &= M_P + 4 M_m + 2 E_{N-m} \\ &= 1189.0 \text{ MeV}. \end{aligned} \quad (33)$$

The calculated mass is in a good agreement with the observed mass,  $1189.4 \pm 0.07 \text{ MeV}$ .

There is N – N hadronic bond between two N's. N has the structure of U – U – U. N – N has a hexagonal structure shown in Fig. 18.

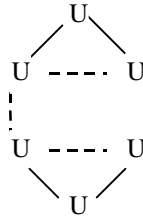


**Fig. 18** The structure of N - N

There are two additional U – U for each N. The total number of U – U bonds between two N's is 4. An example is  $\Lambda_c^+$  (udc) which has the block formula of  $N_2 m_3 U$  with the structure of  $m - N - N - m_2 U$ . The mass of  $\Lambda_c^+$  can be calculated as follows.

$$\begin{aligned} M_{\Lambda_c^+} &= 2M_N + M_U + 3M_m + 4 E_{U-U} + 2 E_{N-m} \\ &= 2285.1 \text{ MeV} \end{aligned} \quad (34)$$

The calculated mass for  $\Lambda_c^+$  is in a good agreement with the observed mass ( $2284.9 \pm 0.6$  MeV). For baryons other than p and n, there are two N-m or P - m bonds per baryon for  $J = \pm 1/2$ , and three bonds for  $J \geq 3/2$ .

Among the particles in the block formula, there are hadronic bonds, but not all particles have hadronic bonds. In the block formula, hadronic bonds appear only among the particles that relate to the particles in the corresponding quark formula. The related particles are the “core” particles that have hadronic bonds. The unrelated particles have no hadronic bonds. In the block formula, for baryons other than p and n, the core particles are P, N, and m. For the mesons consisting of u and d quarks, the core particles are m, U, and N. For the mesons containing one u, d, or s along with s, c, or b, the core particles are U and N, and no hadronic bond exist among m's. For the mesons ( $c \bar{c}$  and  $b \bar{b}$ ), the only hadronic bond is N – N. The occurrences of hadronic bonds are listed in Table 6.

**Table 6.** Hadronic bonds in hadrons

	U –U	m – m	N(P) – m	N –N
Binding energy (MeV)	-26.384	-5.0387	-14.6894	2 U–U per N
Baryons other than n and p			√	√
Mesons with u and d only	√	√		√
Mesons containing one u, d, or s along with s, c, or b	√			√
$c \bar{c}$ or $b \bar{b}$ mesons				√

An example is the difference between  $\pi$  and  $f_0$ . The decay modes of  $f_0$  include the mesons of s quarks from K meson. Consequently, there is no m-m for  $f_0$ . The block formula for  $f_0$  is 14. The mass of  $f_0$  is as follows.

$$\begin{aligned} M &= 14M_m \\ &= 980.4 \text{ MeV} \end{aligned} \quad (35)$$

The observed mass is  $980 \pm 10$  MeV.

In additional to the binding energies for hadronic bonds, hadrons have Coulomb energy (-1.2 MeV) between positive and negative charges and magnetic binding energy ( $\pm 2$ MeV per interaction) for U–U from the constituent quark model [3]. In the constituent quark model, the dipole moment of a hadron can be calculated from the magnetic binding

energy. Since in the block formula, magnetic binding energy becomes a part of hadronic binding energy as shown in Eq (26), magnetic binding energy for other baryons is the difference in magnetic binding energy between a baryon and n or p. If a baryon has a similar dipole moment as p or n, there is no magnetic binding energy for the baryon. An example for Coulomb energy and magnetic binding energy is  $\Lambda$  (uds,  $J=1/2$ ) whose formula is  $Pm_3^-$  with the structure of  $m_2-P-m_1^-$  where "-" denotes negative charge. The dipole moment of  $\Lambda$  is  $-6.13 \mu_N$ , while the dipole moment of proton (P) is  $2.79 \mu_N$  [3]. According to the constituent quark model, this difference in dipole moment represents -6 MeV magnetic binding energy. The Coulomb energy between the positive charge P and the negative charge 1- is  $-1.2$  MeV. The electromagnetic mass for 1- is 4.599 MeV. The mass of  $\Lambda$  is calculated as follows.

$$\begin{aligned} M_\Lambda &= M_P + 3M_m + M_{e.m.} + 2 E_{N-m} + E_{mag} + E_{coul} \\ &= 1116.4 \text{ MeV} \end{aligned} \quad (36)$$

The observed mass is  $1115.7 \pm 0.0006$  MeV.

An example of the dual representation of the quark formula and the block formula as expressed by Eq. (22) is  $\Lambda$  (uds). The quark formula for  $\Lambda$  is  $u'd's'm_3$  with mass of 1169.9 MeV. This mass is matched by the mass of the block formula,  $Pm_3^-$  with the mass of 1152.9 MeV. The final mass of  $\Lambda$  is 1152.9 MeV plus the various binding energies.

Baryons are divided into different groups dependent on their composition of quarks. For examples, the baryons with u, d, and one or no s are in the same group. Each group has one or two base baryons. For baryons, the masses of all other baryons in the same group are separated from the base baryons by electric charge in term electromagnetic mass and the multiple of m [35]. For example, for the group with u, d, and one or no s, the base baryons are n and p. The baryons in the same group are  $Pm_3^-$ ,  $Pm_4$ ,  $Pm_4^-$ ,  $Nm_4^-$ ,  $Pm_7$ ,  $Pm_7^-$ ,  $Nm_7^-$ ,  $Pm_7^-$ , and  $Nm_9$  for  $\Lambda^0$ ,  $\Sigma^+$ ,  $\Sigma^0$ ,  $\Sigma^-$ ,  $\Sigma^+(1385)$ ,  $\Sigma^0(1385)$ ,  $\Sigma^-(1385)$ ,  $\Lambda^0(s_{01})$ , and  $\Lambda^0(D_{03})$ , respectively.

The choice of the base baryon in the same group is dependent on the decay mode. If the dominant decay mode includes p or the decay mode that decays into p, the block formula includes P. If the dominant decay mode includes n, the block formula includes N.

For baryons, the additional types of blocks mark the transition from one group to another group. The addition of U block marks the group with 2 s quarks. The addition of another P marks the group with c quark. The addition of another P marks the group with b quark.

Table 7 is the results of calculation for the masses of baryons selected from Ref. [33]. The hadrons selected are the hadrons with precise observed masses and precise known quantum states such as isospin, spin, and decay mode.

**Table 7.** The masses of baryons

Baryons	I(J <sup>P</sup> )	Quark formula	Block formula	Calculated mass	Observed mass	Difference
<u>udd, uud, uds,</u>						
<u>uus, dds</u>						
n	1/2(1/2 <sup>+</sup> )	udd	U <sub>3</sub>	939.54	939.57	-0.03
p	1/2(1/2 <sup>+</sup> )	uud	U <sub>3</sub> -3e	938.21	938.27	-0.06
Λ <sup>o</sup>	0(1/2 <sup>+</sup> )	u'd's m <sub>3</sub>	Pm <sub>3</sub> -	1116.4	1115.7	0.7
Σ <sup>+</sup>	1(1/2 <sup>+</sup> )	u'u's m <sub>4</sub>	Pm <sub>4</sub>	1189.0	1189.4	-0.4
Σ <sup>o</sup>	1(1/2 <sup>+</sup> )	u'd's m <sub>4</sub>	Pm <sub>4</sub> -	1192.4	1192.6	-0.2
Σ <sup>-</sup>	1(1/2 <sup>+</sup> )	d'd's m <sub>4</sub>	Nm <sub>4</sub> -	1194.9	1197.4	-2.5
Σ <sup>+</sup> (1385)	1(3/2 <sup>+</sup> )	u'u's m <sub>7</sub>	Pm <sub>7</sub>	1384.4	1382.8	1.6
Σ <sup>o</sup> (1385)	1(3/2 <sup>+</sup> )	u'd's m <sub>7</sub>	Pm <sub>7</sub> -	1381.8	1383.7	-1.9
Σ <sup>-</sup> (1385)	1(3/2 <sup>+</sup> )	d'd's m <sub>7</sub>	Nm <sub>7</sub> -	1390.3	1387.2	3.1
Λ <sup>o</sup> (S <sub>01</sub> )	0(1/2 <sup>-</sup> )	u'd's m <sub>7</sub>	Pm <sub>7</sub> -	1402.5	1406.0	-3.5
Λ <sup>o</sup> (D <sub>03</sub> )	0(3/2 <sup>-</sup> )	u'd's m <sub>9</sub>	Nm <sub>9</sub>	1525.7	1519.5	6.2
<u>uss, dss</u>						
Ξ <sup>o</sup>	1/2(1/2 <sup>+</sup> )	u'ss	PmU-	1314.3	1314.8	-0.5
Ξ <sup>-</sup>	1/2(1/2 <sup>+</sup> )	d'ss	Ξ <sup>o</sup> -	1318.2	1321.3	-3.1
Ξ <sup>o</sup> (1530)	1/2(3/2 <sup>+</sup> )	u'ss m <sub>4</sub>	Ξ <sup>o</sup> m <sub>3</sub> +-	1532.9	1531.8	1.1
Ξ <sup>-</sup> (1530)	1/2(3/2 <sup>+</sup> )	d'ss m <sub>4</sub>	Ξ <sup>o</sup> m <sub>3</sub> +-	1536.3	1535.0	1.3
Ξ <sup>o</sup> (1820)	1/2(3/2 <sup>-</sup> )	u'ss m <sub>8</sub>	Ξ <sup>o</sup> m <sub>7</sub> +-	1813.0	1823.0	-10.0
<u>udc, ddc, uuc</u>						
Λ <sup>+</sup> <sub>c</sub>	0(1/2 <sup>+</sup> )	u'd'c m <sub>5</sub>	P <sub>2</sub> m <sub>3</sub> U	2282.5	2284.9	-2.4
Σ <sup>+</sup> <sub>c</sub> (2455)	1(1/2 <sup>+</sup> )	u'd'c m <sub>7</sub>	P <sub>2</sub> m <sub>4</sub> X+-	2449.9	2451.3	-1.4
Σ <sup>o</sup> <sub>c</sub> (2455)	1(1/2 <sup>+</sup> )	d'd'c m <sub>7</sub>	Σ <sup>+</sup> <sub>c</sub> (2455)-	2455.9	2452.2	3.7
Σ <sup>+</sup> <sub>c</sub> (2455)	1(1/2 <sup>+</sup> )	u'u'c m <sub>7</sub>	Σ <sup>+</sup> <sub>c</sub> (2455)+	2455.9	2452.6	3.3
Σ <sup>+</sup> <sub>c</sub> (2520)	1(3/2 <sup>+</sup> )	u'd'c m <sub>8</sub>	Σ <sup>+</sup> <sub>c</sub> (2455)m	2521.3	2515.9	5.4
Σ <sup>o</sup> <sub>c</sub> (2520)	1(3/2 <sup>+</sup> )	d'd'c m <sub>8</sub>	Σ <sup>+</sup> <sub>c</sub> (2455)m	2525.9	2517.5	8.4
Σ <sup>+</sup> <sub>c</sub> (2520)	1(3/2 <sup>+</sup> )	u'u'c m <sub>8</sub>	Σ <sup>+</sup> <sub>c</sub> (2455)m+	2525.9	2519.4	6.5
Λ <sup>+</sup> <sub>c</sub>	0(1/2 <sup>-</sup> )	u'd'c m <sub>9</sub>	Σ <sup>+</sup> <sub>c</sub> (2455)m <sub>2</sub> -	2591.4	2593.9	-2.5
<u>usc, dsc</u>						
Ξ <sup>+</sup> <sub>c</sub>	1/2(1/2 <sup>+</sup> )	u'sc m <sub>2</sub>	P <sub>2</sub> mU <sub>2</sub> +	2473.2	2477.8	11.5
Ξ <sup>o</sup> <sub>c</sub>	1/2(1/2 <sup>+</sup> )	d'sc m <sub>2</sub>	Ξ <sup>+</sup> <sub>c</sub> -	2470.9	2471.8	-0.9
Ξ <sup>+</sup> <sub>c</sub>	1/2(1/2 <sup>+</sup> )	u'sc m <sub>3</sub>	P <sub>2</sub> mXU+	2567.2	2574.1	-6.9
Ξ <sup>o</sup> <sub>c</sub>	1/2(1/2 <sup>+</sup> )	d'sc m <sub>3</sub>	Ξ <sup>+</sup> <sub>c</sub> -	2578.7	2578.8	-0.1
Ξ <sup>+</sup> <sub>c</sub> (2645)	1/2(3/2 <sup>+</sup> )	u'sc m <sub>5</sub>	Ξ <sup>+</sup> <sub>c</sub> m	2644.1	2647.4	-3.3
Ξ <sup>o</sup> <sub>c</sub> (2645)	1/2(3/2 <sup>+</sup> )	d'sc m <sub>7</sub>	Ξ <sup>+</sup> <sub>c</sub> m-	2648.7	2645.0	3.7
Ξ <sup>+</sup> <sub>c</sub> (2790)	1/2(1/2 <sup>-</sup> )	u'sc m <sub>7</sub>	Ξ <sup>+</sup> <sub>c</sub> m <sub>3</sub>	2784.2	2790.0	-5.8
Ξ <sup>o</sup> <sub>c</sub> (2790)	1/2(1/2 <sup>-</sup> )	d'sc m <sub>7</sub>	Ξ <sup>+</sup> <sub>c</sub> m <sub>3</sub> -	2788.8	2790.0	-1.2
Ξ <sup>+</sup> <sub>c</sub> (2815)	1/2(3/2 <sup>-</sup> )	u'sc m <sub>7</sub>	Ξ <sup>+</sup> <sub>c</sub> m <sub>5</sub>	2816.4	2814.9	1.5
Ξ <sup>o</sup> <sub>c</sub> (2815)	1/2(3/2 <sup>-</sup> )	d'sc m <sub>7</sub>	Ξ <sup>+</sup> <sub>c</sub> m <sub>5</sub> -	2821.0	2819.0	2.0
<u>sss, ssc</u>						
Ω <sup>-</sup>	0(3/2 <sup>+</sup> )	sss	PXU+-	1667.8	1672.5	-4.7
Ω <sup>o</sup> <sub>c</sub>	0(1/2 <sup>+</sup> )	ssc	P <sub>2</sub> m <sub>3</sub> XU	2701.4	2697.5	3.9
<u>udb</u>						
Λ <sup>o</sup> <sub>b</sub>	0(1/2 <sup>+</sup> )	u'd'b m	P <sub>3</sub> U <sub>9</sub> -	5638.0	5624.0	14.0

Light unflavored mesons have zero strange, charm, and bottom numbers. The mesons are divided into different groups dependent on the decay mode. There are three different types of the quark formula for light unflavored mesons. The first group involves the decay mode whose products are all leptons or all mesons with u and d quarks. The quark formula in the first group consists of  $m, u', d', u,$  and  $d$  quarks. The second group involves the decay mode whose products are u, d, and leptons in the major decay products, s is in the minor decay products. The quark formula in the second group consists of  $m, u', d', s', u, d,$  and  $s$  quarks. The most common quark formula for such mesons is  $uds$ , which is essentially  $\frac{1}{2}(u \bar{u} d \bar{d} s \bar{s})$ . The third group involves the decay mode whose decay products are mostly the mesons with s quark. The quark formula in the third group consists of  $m$  's and  $s$  quarks. When  $J = 0$ , the quark formula includes  $m$  's and hybrid quarks ( $u', d',$  and  $s'$ ). When  $J > 0$ , the quark formula includes  $m$  's and vector quarks ( $u, d,$  and  $s$ ).

Each group has one or more base mesons. In the same group, the masses of the base meson and the next meson with the same spin (J) with the difference in isospin (I) = 0 and  $\pm 1$ , or with the same isospin with the difference in  $J = 0$  and  $\pm 1$  are separated by the multiples of  $m_2, X, U,$  and electric mass. The third meson and the second meson again are separated by the multiples of  $m_2, X, U, mX, mU,$  and electric mass. For example, the group of  $\pi^0, \eta(547), \eta'(958), \eta(1295), \pi(1300),$  and  $f_0(1500)$  are represented by  $m_2, \pi^0(135)X^{+-}, \eta(547)X^{+-}, \eta'(958)U, \eta'(958)U^{+-},$  and  $\eta'(958)m_2X^{+-}$ , respectively, where  $\pi^0$  is the base meson.

The block formula includes  $\pi_{1/2}$  's, U, and N.  $m - m$  hadronic bond exists in the quark formula with u and d quarks, and does not exist in the quark formula with s quark. U - U bond exists in all formula.

The result of calculated masses for light unflavored mesons is listed in Table 8.

**Table 8.** Light unflavored mesons

Meson	I (J <sup>pc</sup> )	Quark formula	Block formula	Calculated mass.	Observed mass	Difference
<u>J = 0, only u, d, or lepton in decay mode</u>						
$\pi^0$ (135)	1 (0 <sup>+</sup> )	$m_2$	$m_2$	135.0	134.98	0.04
$\pi^\pm$ (140)	1 (0 <sup>-</sup> )	$m_{2\pm}$	$m_{2\pm}$	139.6	139.57	0.04
$\eta$ (547)	0 (0 <sup>+</sup> )	$u'd'm_2$	$\pi^0$ (135)X+-	548.0	547.3	0.7
$\eta'$ (958)	0 (0 <sup>+</sup> )	$u'u'd'd'm_3$	$\eta$ (547)X+-	960.3	957.8	2.5
$\eta$ (1295)	0 (0 <sup>+</sup> )	$u'u'u'd'd'm_2$	$\eta'$ (958)U	1288.6	1293.0	-4.4
$\pi$ (1300)	1 (0 <sup>+</sup> )	$u'u'u'd'd'm_2$	$\eta'$ (958)U+-	1296.6	1300.0	-3.4
<u>J &gt; 0, only u, d, or lepton in decay modes</u>						
$\rho$ (770)	1 (1 <sup>-</sup> )	$udm_2$	$m_2U_2$	770.2	771.1	-0.9
$\omega$ (782)	0 (1 <sup>-</sup> )	$udm_2$	$\rho$ (770)+-	779.1	782.6	-3.5
$h_1$ (1170)	0 (1 <sup>+</sup> )	$udm_8$	$\omega$ (770)X	1176.1	1170.0	6.1
$\omega$ (1420)	0 (1 <sup>-</sup> )	$uuddm_2$	$\omega$ (782)U <sub>2</sub>	1417.8	1419.0	-1.2
$\omega$ (1650)	0 (1 <sup>-</sup> )	$uuddm_5$	$\omega$ (782)m <sub>2</sub> XU	1653.4	1649.0	4.4
<u>J = 0, u and d in major decay modes, s in minor decay modes</u>						
$f_0$ (980)	0 (0 <sup>++</sup> )	$u'd's'm_4$	$m_2X_2$	980.4	980.0	0.4
$a_0$ (980)	1 (0 <sup>++</sup> )	$u'd's'm_4$	$m_2X_2+-$	988.4	984.0	4.4
$a_0$ (1450)	1 (0 <sup>++</sup> )	$u'u'd'd's's'm$	$a_0$ (980)mX	1474.2	1474.0	0.2
$f_0$ (1500)	0 (0 <sup>++</sup> )	$u'u'd'd's's'm_2$	$m_2XU_{3+-}$	1507.7	1507.0	0.7
$\pi$ (1800)	1 (0 <sup>+</sup> )	$u'u'd'd's's'm_5$	$a_0$ (1450)U	1804.8	1801.0	3.8
<u>J &gt; 0, u and d in major decay modes, s in minor decay mode</u>						
$a_1$ (1260)	1 (1 <sup>++</sup> )	$udsm$	$m_4U_{3+-}$	1227.6	1230.0	-2.4
$b_1$ (1235)	1 (1 <sup>+</sup> )	$udsm$	$U_4$	1243.9	1239.5	4.4
$f_2$ (1270)	0 (2 <sup>++</sup> )	$udsm$	$U_2 m_3X+-$	1273.4	1275.4	-2.0
$f_1$ (1285)	0 (1 <sup>++</sup> )	$udsm$	$f_2$ (1270)+-	1283.4	1281.9	1.5
$a_2$ (1320)	1 (2 <sup>++</sup> )	$udsm$	$m_2X_2U+-$	1319.1	1318.0	1.1
$\rho$ (1450)	1 (1 <sup>-</sup> )	$udsm_3$	$a_0$ (980)m <sub>2</sub> U+-	1457.8	1465.0	-7.2
$\pi_2$ (1670)	1 (2 <sup>+</sup> )	$udsm_8$	$XU_{3+-}$	1672.1	1670.0	2.1
$\omega_3$ (1670)	0 (3 <sup>-</sup> )	$udsm_7$	$XU_3$	1664.1	1667.0	-2.9
$\rho_3$ (1690)	1 (3 <sup>-</sup> )	$udsm_7$	$X_{4+-}$	1688.6	1691.0	-2.4
$\rho$ (1700)	1 (1 <sup>-</sup> )	$udsm_7$	$a_0$ (980)m <sub>4</sub> X	1692.3	1700.0	-7.7
$a_4$ (2040)	1 (4 <sup>++</sup> )	$udsm_{11}$	$X_4U$	2011.4	2011.0	0.4
$f_4$ (2050)	0 (4 <sup>++</sup> )	$udsm_{11}$	$a_4$ (2040)+-	2019.0	2025.0	-6.0
<u>s in major decay modes</u>						
$\eta$ (1440)	0 (0 <sup>+</sup> )	$u'u'd'd's's' m$	$mXU_{3+-}$	1437.7	1440.0	-2.3
$f_0$ (1710)	0 (0 <sup>++</sup> )	$u'u'd'd's's'm_5$	$\eta$ (1440)m <sub>4</sub>	1720.1	1710.0	10.1
$\Phi$ (1020)	0 (1 <sup>-</sup> )	$ssm_1$	$mU_{3+-}$	1017.6	1019.4	-1.8
$f_1$ (1420)	0 (1 <sup>++</sup> )	$ssm_5$	$mXU_3$	1429.7	1426.3	3.4
$f_2$ (1525)	0 (2 <sup>++</sup> )	$ssm_7$	$m_4U_4$	1524.0	1525.0	-1.0
$\Phi$ (1680)	0 (1 <sup>-</sup> )	$ssm_9$	$f_2(1525)m_{2+-}$	1674.2	1680.0	-5.8
$\Phi_3$ (1850)	0 (3 <sup>-</sup> )	$ss m_{12}$	$U_6$	1852.7	1854.0	-1.3
$f_2$ (2010)	0 (2 <sup>++</sup> )	$ss m_{13}$	$\Phi_3$ (1850)m <sub>2</sub> +-	2002.0	2011.0	-9.0
$f_2$ (2300)	0 (2 <sup>++</sup> )	$sssm_2$	$f_2(1525)m_2U_2$	2300.2	2297.0	3.2
$f_2$ (2340)	0 (2 <sup>++</sup> )	$sssm_2$	$f_2(2010)U$	2341.8	2339.0	2.8



**Table 9.** Light unflavored mesons

$J^{pc}$	$I = 1$			$I = 0$		
	<b>meson</b>	<b>decay</b>	<b>block</b>	<b>meson</b>	<b>decay</b>	<b>block</b>
$0^+$	$\pi^0(135)$	lepton	$m_2$	$\eta(547)$	u,d	$\pi^0(135)X_{+-}$
	$\pi^\pm(140)$	lepton	$m_{2\pm}$	$\eta'(958)$	u,d	$\eta(547)X_{+-}$
	$\pi(1300)$	u,d	$\eta'(958)U_{+-}$	$\eta(1295)$	u,d	$\eta'(958)U$
	$\pi(1800)$	u,d,s	$a_0(1450)U$	$\eta(1440)$	s,d,u	$mXU_{3+-}$
$1^-$	$\rho(770)$	u,d	$m_2U_2$	$\omega(782)$	u,d	$\rho(770)_{+-}$
	$\rho(1450)$	u,d,s	$a_0(980)m_2U_{+-}$	$\omega(1420)$	u,d	$\omega(782)U_2$
	$\rho(1700)$	u,d,s	$a_0(980)m_4X$	$\omega(1650)$	u,d	$\omega(782)m_2XU$
				$\Phi(1020)$	s,u,d	$mU_{3+-}$
			$\Phi(1680)$	s,u,d	$f'_2(1525)m_{2+-}$	
$0^{++}$	$a_0(980)$	u,d,s	$m_2X_{2+-}$	$f_0(980)$	u,d,s	$m_2X_2$
	$a_0(1450)$	u,d,s	$a_0(980)mX$	$f_0(1500)$	u,d,s	$m_2XU_{3+-}$
				$f_0(1710)$	s,u,d	$\eta(1440)m_4$
$1^{++}$	$a_1(1260)$	u,d,s	$m_4U_{3+-}$	$f_1(1285)$	u,d,s	$f_2(1270)_{+-}$
				$f_1(1420)$	s,d,u	$mXU_3$
$1^{+-}$	$b_1(1235)$	u,d,s	$U_4$	$h_1(1170)$	u,d	$\omega(770)X$
$2^{++}$	$a_2(1320)$	u,d,s	$m_2X_2U_{+-}$	$f_2(1270)$	u,d,s	$U_2m_3X_{+-}$
				$f_2'(1525)$	s,u,d	$m_4U_4$
				$f_2(2010)$	s,u,d	$\Phi(1850)m_{2+-}$
				$f_2(2300)$	s,u,d	$f_2'(1525)m_2U_2$
				$f_2(2340)$	s,u,d	$f_2(2010)U$
$2^+$	$\pi_2(1670)$	u,d,s	$XU_{3+-}$			
$3^-$	$\rho_3(1690)$	u,d,s	$X_{4+-}$	$\omega_3(1670)$	u,d,s	$XU_3$
				$\Phi_3(1850)$	s,u,d	$U_6$
$4^{++}$	$a_4(2040)$	u,d,s	$X_4U$	$f_4(2050)$	u,d,s	$a_4(2040)_{+-}$

In Table 9, the decay u, d, s has s as a minor decay mode, while the decay s, d, u has s as a major decay mode. The two major groups in the block formulas in Table 8 are the  $m_2$  base group ( $m_2$ ,  $m_2U_2$ , and  $m_2X_2$ ) and  $U_3$  base group ( $mU_3$ ,  $m_4U_3$ ,  $XU_3$ ,  $mXU_3$ , and  $m_2XU_3$ ). The  $m_2$  group represents mesons involving mostly pseudoscalar and vector u and d. The  $U_3$  (939.5 MeV) group represents mesons involving s quark and vector and pseudoscalar u and d ( $u + s + m = 959.1\text{MeV}$ ).

The result of the mass calculation for the mesons consisting of u, d, or s with s, c, or b is listed in Table 10.

**Table 10.** Mesons with s, c, and b

Meson	$J^{PC}$	Quark formula	Block formula	Calculate d mass.	Observed mass	Difference
<u>Light strange mesons</u>						
$K^\pm$ (494)	$0^-$	u's'	$mX^\pm$	494.8	493.7	1.1
$K^0$ (498)	$0^-$	d's'	$mX^{+-}$	498.2	497.7	0.5
$K^*_0$ (1430)	$0^+$	d'd's's'm <sub>6</sub>	$K^0(498) m_4 U_2$	1413.0	1412.0	1.0
$K^*$ (892) <sup>±</sup>	$1^-$	us	$m_2 XU^\pm$	895.6	891.6	4.0
$K^*$ (892) <sup>0</sup>	$1^-$	ds	$m_2 XU^{+-}$	899.0	896.1	2.9
$K_1$ (1270)	$1^+$	dsm <sub>6</sub>	$K^0(498) m_2 U_2$	1272.9	1273.0	-0.1
$K_1$ (1400)	$1^+$	dsm <sub>8</sub>	$K_1(1270) m_2$	1413.1	1402.0	11.1
$K^*$ (1410)	$1^-$	dsm <sub>8</sub>	$K^0(498) m_4 U_2$	1413.0	1414.0	-1.0
$K^*_2(1430)^\pm$	$2^+$	usm <sub>8</sub>	$K_1(1270) m_2^\pm$	1417.6	1432.4	-8.0
$K^*_2(1430)^0$	$2^+$	dsm <sub>8</sub>	$K^*_2(1430)^\pm$	1430.2	1436.9	2.2
$K^*$ (1680)	$1^-$	ddss	$K^0(498) m_4 U_3$	1717.3	1717.0	0.3
$K_2$ (1770)	$2^-$	ddss	$K^*_2((1430)^0) U^{+-}$	1771.2	1772.4	-0.6
$K_3^*$ (1780)	$3^-$	ddss	$K_2(1770)^{+-}$	1782.2	1776.0	6.2
$K_2$ (1820)	$2^-$	ddssm	$K_1(1400) X$	1822.2	1816.0	6.2
$K_4^*$ (2045)	$4^+$	ddssm <sub>4</sub>	$K^*_3(1780) m_4$	2056.1	2045.0	11.1
<u>Charmed mesons</u>						
$D(1865)^0$	$0^-$	u'cm	$U_6^{+-}$	1860.7	1864.5	-3.8
$D(1869)^\pm$	$0^-$	d'cm	$D(1864)^\circ^\pm$	1869.1	1869.3	-0.2
$D^*$ (2007) <sup>0</sup>	$1^-$	ucm <sub>6</sub>	$D^0(1864)^\circ m_2$	2004.6	2006.7	-2.1
$D^*$ (2010) <sup>±</sup>	$1^-$	dcm <sub>6</sub>	$D(1869)^\pm m_2$	2009.4	2010	-0.6
$D_1$ (2420) <sup>0</sup>	$1^+$	ucm <sub>12</sub>	$D^*(2010)^\pm X$	2430.2	2422.2	8.0
$D_2^*$ (2460) <sup>0</sup>	$2^+$	ucm <sub>14</sub>	$U_8$	2461.5	2458.9	2.6
$D_2^*$ (2460) <sup>±</sup>	$2^+$	dcm <sub>14</sub>	$U_8^\pm$	2466.1	2459	7.1
<u>Charmed strange mesons</u>						
$D_s^\pm$	$0^-$	s'cm	$U_5 X^\pm$	1973.1	1968.5	4.6
$D_s^*^\pm$	$1^-$	sc-m <sub>2</sub>	$D_s^\pm m_2$	2113.1	2112.4	0.7
$D_{s1}(2536)^\pm$	$1^+$	scm <sub>13</sub>	$D_s^*^\pm X$	2537.2	2535.4	1.8
$D_{sJ}(2573)^\pm$	$2^+$	scm <sub>15</sub>	$U_6 X^\pm$	2581.8	2572.4	9.4
<u>Bottom mesons</u>						
$B^\pm$	$0^-$	u'b	$mU_{17}^\pm$	5275.6	5279.0	4.1
$B^0$	$0^-$	d'b	$mU_{17}^{+-}$	5279.0	5279.4	-0.9
$B^*$	$1^-$	dbm <sub>6</sub>	$XU_{16}^{+-}$	5324.7	5325	-0.3
$B_s$	$0^-$	s'b	$mXU_{13} N^{+-}$	5368.4	5369.6	-1.2

The quark formula for these mesons contains m's, u', d', s', u, d, s, c, and b. The quark formula for the mesons with J = 0 contains m, hybrid quarks (u', d', and s'), c, and b quarks. The quark formula with J > 0 contains m's and vector quarks (u, d, s, c, and b). The block formula consists of m, U, and N. There is no m – m bond. There are U – U and N – N bonds. For example, the mass of B<sub>s</sub> (mXU<sub>13</sub>N<sup>+-</sup>) with the observed mass as 5369.6 ± 2 MeV is calculated as follows.

$$\begin{aligned} M &= M_N + 7M_m + 13M_U + 12 M_{U-U} + 2M_{e,m} \\ &= 5368.4 \text{ MeV} \end{aligned} \quad (38)$$

The result of mass calculation for c  $\bar{c}$  and b  $\bar{b}$  mesons is listed in Table 11.

**Table 11.** c  $\bar{c}$  and b  $\bar{b}$  mesons

Meson	J <sup>PC</sup>	Quark formula	Block formula	Calculated mass.	Observed mass	Difference
<u>c <math>\bar{c}</math> mesons</u>						
$\eta_c$ (1s)	0 <sup>+</sup>	cc m <sub>6</sub>	U <sub>9</sub>	2976.9	2979.7	-2.8
J/ $\psi$	1 <sup>-</sup>	cc m <sub>3</sub>	N <sub>2</sub> U <sub>4</sub>	3096.7	3096.9	-0.2
$\chi_c$ (1p)	0 <sup>++</sup>	cc	$\eta_c$ (1s)X <sup>+-</sup>	3408.0	3415.1	-7.2
$\chi_{c1}$ (1p)	1 <sup>++</sup>	cc m <sub>3</sub>	J/ $\psi$ X	3517.1	3510.5	6.6
$\chi_{c2}$ (1p)	2 <sup>++</sup>	cc m <sub>2</sub>	$\chi_{c1}$ (1p) m <sub>2</sub>	3555.1	3556.2	-1.0
U <sub>2s</sub>	1 <sup>-</sup>	cc m <sub>4</sub>	$\eta_c$ (1s)m <sub>2</sub> X <sub>2+-</sub>	3688.0	3686	2.0
$\psi$ (3770)	1 <sup>-</sup>	cc m <sub>7</sub>	J/ $\psi$ U <sub>2</sub>	3758.4	3769.9	-11.5
$\psi$ (4040)	1 <sup>-</sup>	cc m <sub>11</sub>	J/ $\psi$ N	4036.5	4040	-3.5
$\psi$ (4160)	1 <sup>-</sup>	cc m <sub>13</sub>	J/ $\psi$ XU <sub>2+-</sub>	4160.2	4159	1.2
$\psi$ (4415)	1 <sup>-</sup>	cc m <sub>15</sub>	$\chi_c$ (1p)U <sub>3+-</sub>	4415.4	4415	0.4
<u>b <math>\bar{b}</math> mesons</u>						
$\Upsilon$ (1s)	1 <sup>-</sup>	bb m <sub>10</sub>	N <sub>9</sub> U <sub>3</sub> mX	9463.7	9460.3	3.4
$\chi_b$ (1p)	0 <sup>++</sup>	bb m <sub>4</sub>	N <sub>10</sub> U <sub>3</sub>	9860.3	9859.9	0.4
$\chi_{b1}$ (1p)	1 <sup>++</sup>	bb m <sub>4</sub>	$\Upsilon$ (1s) X <sup>+-</sup>	9888.5	9892.7	-4.2
$\chi_{b2}$ (1p)	2 <sup>++</sup>	bb m <sub>4</sub>	$\chi_{b1}$ (1p) +-	9900.7	9912.6	-11.9
$\Upsilon$ (2s)	1 <sup>-</sup>	bb m <sub>2</sub>	$\chi_b$ (1p)m <sub>2</sub>	10032.8	10023.3	9.5
$\chi_{b0}$ (2p)	0 <sup>++</sup>	bb m <sub>1</sub>	$\chi_b$ (1p)U <sup>+-</sup>	10231.5	10232.1	-0.6
$\chi_{b1}$ (2p)	1 <sup>++</sup>	bb m <sub>1</sub>	$\chi_{b2}$ (1p)U	10251.1	10255.2	-3.8
$\chi_{b2}$ (2p)	2 <sup>++</sup>	bb m <sub>2</sub>	$\chi_{b1}$ (2p)+-	10263.2	10268.5	-5.3
$\Upsilon$ (3s)	1 <sup>-</sup>	bb m <sub>3</sub>	$\Upsilon$ (2s)U	10354.1	10355.2	-1.1
$\Upsilon$ (4s)	1 <sup>-</sup>	bb m <sub>6</sub>	$\chi_{b1}$ (2p)U	10586.0	10580.0	6.0
$\Upsilon$ (10860)	1 <sup>-</sup>	bb m <sub>10</sub>	$\Upsilon$ (4s)m <sub>4</sub>	10860.1	10865	-4.9
$\Upsilon$ (11020)	1 <sup>-</sup>	bb m <sub>12</sub>	$\Upsilon$ (3s)U <sub>2</sub>	11016.7	11019	-2.3

The quark formula contains c or b. Since c and b are high mass quarks unlike the low mass u and d quarks that relate to m, the series actually starts from a negative m. The

block formula contains  $m$ 's,  $U$ , and  $N$ . The only hadronic bond is  $N - N$ . An example is  $J/\psi$  ( $N_2 U_4$ ) whose mass ( $3096.9 \pm 0.04$  MeV) is calculated as follows.

$$\begin{aligned} M &= 2 M_N + 4 M_U + 4 M_{U-U} \\ &= 3096.7 \text{ MeV} \end{aligned} \tag{37}$$

## 11. Conclusion

The foundation of the cosmic evolution is the multiverse, which consists of consists of two variable components: varying dimensions and varying object-space. Different universes in the multiverse have different variables from these two variable components. Varying dimensions consist of varying space-time and mass dimensions. The varying speed of light is quantized by varying space-time dimension, resulting in varying mass in terms of varying mass dimension. The transformation of varying mass in terms of varying mass dimension is by varying supersymmetry, relating to dimensional fermions and bosons. Four objects (string, membrane, particle, and particle-wave) and four spaces (blank space, fermion space, boson space, and exclusion space) constitute varying object-space.

The evolution of our expanding universe involves four stages: the pre-universe, the pre-expanding universe, the mixed pre-expanding universe, and the expanding universe. In the pre-universe, object and vacuum take turn to exist equally at the same location. It is an equilibrium state between vacuum and the pair of ten-dimensional superstring and anti-superstring with a non-zero vacuum energy. The vacuum fluctuation (Figs. 1, 2, 3, and 4) results in the pre-expanding universe with the chiral boundary positive charged 9-brane and the chiral boundary negative charged 9-antibrane separated by pregravity (the predecessor of gravity) and anti-pregravity. The collapse and the bounce of the pre-expanding universe result in the generation of the achiral mixed 9-particle with the multiple dimensional Kaluza-Klein structure, achiral pregravity, achiral anti-pregraivty, and zero vacuum energy (Fig. 5).

The decrease in vacuum energy leads to the fractionalization of mixed 9-particles into mixed particles with lower space-time and mass dimensions, resulting in the cosmic expansion. The two modes, the slow mode and the quick mode, of the cosmic expansion lead to two universes, the hidden universe and the observable universe, respectively as shown in Fig. 6. In the slow mode, the space-time and mass dimensions decrease and then increase gradually and sequentially. In the quick mode, the space-time dimension decreases to four immediately, and the fractionalization of mixed 9-particles completes immediately by renormalization into real mass dimensions and virtual mass dimensions. During renormalization, exclusion space appears, and the inflationary expansion occurs. After the inflation, the cooling of the universe is accomplished by the non-inflationary decelerating expansion, resulting in the big bang, cosmic radiation, elementary particles, dark matter, entropy, force fields, and quantum mechanics. The cosmic evolution involving objects and spaces is shown in Fig. 7.

In the space theory of quantum mechanics, quantum mechanics is the interaction of four spaces. Wavefunction is the combination of boson space and exclusion space to generate the uncertainty about the existence of object at any specific point in space. The

collapse of wavefunction is the disappearance of the combination of boson space and exclusion space and the appearance of fermion space that contains only one object. Quantum mechanics explained by spaces is shown in Fig. 8.

In the expanding universe, the hidden universe and the observable universe are incompatible until the particles in the hidden universe are converted to the  $4D$  particles compatible to the  $4D$  particles in the observable universe. The compatible universes lead to the emergence of dark energy that causes accelerated cosmic expansion in the observable universe as shown in Fig. 9. The increase in the fine structure constant relates to the emergence of this time dependent dark energy. The contraction of the hidden universe from the  $4D$  particle to the  $5D$  particle brings about the contraction in the observable universe. Eventually, both universes are back to the mixed pre-expanding universe to start another cycle as shown in Fig. 10.

The observable universe is the Milky Universe. In the Milky Universe model, baryonic matter with four-mass dimension is incompatible with dark matter with higher mass-dimensions. Both of them are compatible with cosmic radiation. The incompatibility increases with the increasing size of the universe. Such incompatibility brings about the formation of inhomogeneous structure (anisotropies in the CMB) where the baryonic matter domains surrounded by the dark matter halos as oil droplets surrounded by water in emulsion. The gravitational interaction between baryonic matter and dark matter can be described by the Modified Newtonian Dynamics (MOND) (Fig. 11). The five periods (Fig. 15) of baryonic structure development in the order of increasing incompatibility between baryonic matter and dark matter are the free baryonic matter, the baryonic droplet, the galaxy, the cluster, and the supercluster periods. The transition to the baryonic droplet generates density perturbation in the CMB. The transition from the baryonic droplet to galaxy is through the big eruption for the formations of the first-generation galaxies, including elliptical, normal spiral (Fig. 13), barred spiral (Fig. 14), irregular, and dwarf spheroidal galaxies. The transitions to cluster and supercluster are the mergers and interactions of galaxies for the formation of the second-generation galaxies, including modified giant ellipticals, cD, evolved S0, dwarf elliptical, BCD, and tidal dwarf galaxies. The universe now is in the early part of the supercluster period. The whole observable expanding universe behaves as one unit of emulsion with increasing incompatibility between dark matter and baryonic matter.

The model for baryonic matter is the periodic table of elementary particles. There is duality between the cosmic evolution and physical laws. Derived from the cosmic evolution, baryonic matter has the dimensional orbital that resembles to atomic orbital. The dimensional orbital constitutes the periodic table of elementary particles (Fig. 17 and Table 2) to account for all leptons, quarks, and gauge bosons. Based on the quantized mass formulas (Eq. (11) and Eq. (19)), the calculated masses (Tables 1 and 3) of gauge bosons, leptons, and quarks derived from the periodic table are in good agreement with the observed values. For example, the calculated mass (176.5 GeV) of the top quark has an excellent agreement with the observed mass ( $174.3 \pm 5.1$  GeV).

A hadron can be represented by the quark formula (Table 4) and the basic quark formula (Table 5). The quark formula consists of all quarks, pseudoscalar quark in pion, and the hybrid quarks. The basic quark formula consists of the lowest mass quarks. The relation

between these two formulas is expressed by Eq. (22). As a molecule is the composite of atoms with chemical bonds, a hadron is the composite of elementary particles with "hadronic bonds" (Table 6) which are the overlappings of the auxiliary dimensional orbits. The calculated masses (Tables 7, 8, 10, and 11) of hadrons are in good agreement with the observed values. For examples, the calculated masses for neutron and pion are 939.54 and 135.01MeV in excellent agreement with the observed masses, 939.57 and 134.98 MeV, respectively. The overall standard deviation between the calculated masses and the observed masses for all hadrons (128 hadrons) is 4.7 MeV, comparing to  $\pm 13.9$  MeV, the average observed error for the masses of the hadrons. The masses of gauge bosons, leptons, quarks, and hadrons can be calculated using only four known constants: the number of the extra spatial dimensions in the eleven dimensional membrane, the mass of electron, the mass of  $Z^0$ , and  $\alpha_e$ .

In conclusion, the cosmic evolution takes place in the multiverse, we live in the Milky Universe, and our baryonic matter follows the periodic table of elementary particles. This whole picture of Nature gives rise to viable cosmology, detailed explanation of astronomy, and accurate calculation of the masses of elementary particles and hadrons.

## References

- \* chung@wayne.edu
- [1] D. Chung, hep-th/0111147, D. Chung, *Speculations in Science and Technology* 20 (1997) 259; *Speculations in Science and Technology* 21(1999) 277
  - [2] A.O. Barut, *Phys. Rev. Lett.* 42.(1979) 1251
  - [3] M.H. MacGregor, *Nuovo Cimento A*, 103, 983 (1990)
  - [4] G. Amelino-Camelia, *Int. J. Mod. Phys. D*11 (2002) 35 [gr-qc/0012051]; *Phys. Letts. B*510 (2001) 255 [hep-th/0012238]; J Barrow, gr-qc/0211074; G. Ellis and J. Uzan, gr-qc/0305099; J. Magueijo, astro-ph/0305457
  - [5] L. Randall and R. Sundrum, *Nucl. Phys.* **B557** (1999) 79; *Phys. Rev. Lett.* **83** (1999) 3370 ; *Phys. Rev. Lett.* **83** (1999) 4690
  - [6] P. Horava and E. Witten, *Nucl. Phys.* **B475** (1996) 94 [hep-th/9603142].
  - [7] J. Khoury, B. A. Ovrut, P. J. Steinhardt, and N. Turok, hep-th/0103239; R. Kallosh, L. Kofman, and A. Linde, hep-th/0104073; S. Rasanen, hep-th/0111279.
  - [8] G. Dvali, Q. Shafi, and S. Solganik, hep-th/0105203; C. P. Burgess, M. Majumdar, D. Nolte, F. Quevedo, G. Rajesh, and R. J. Zhang, hep-th/0105204.
  - [9] M. Bucher, hep-th/0107148; A. Nornov, hep-th/0109090; M.F. Parry, D. A. Steer, hep-th/0109207, D. Langlois, K. Maeda, D. Wards, gr-qc/0111013; J. Garriga, T. Tanaka, hep-th/0112028, S. Mukherji and M. Peloso, hep-th/0205180, P. Brax and D. A. Steer, hep-th/0207280, Y. S. Myung, hep-th/0208086
  - [10] J. Khoury, B. A. Ovrut, N. Seiberg, P. J. Steinhardt, and N. Turok, hep-th/0108187; P. J. Steinhardt, and N. Turok, hep-th/0111098; P. J. Steinhardt, and N. Turok, astro-ph/0112537; J. Martin, P. Peter, N. Pinto-Neto, and D. Schwarz, hep-th/0112128; P. Steinhardt and N. Turok, astro-ph/0204479, R. Dave, R. R. Caldwell, P. J. Steinhardt, astro-ph/0206372

- [11] A. H. Guth, Phys. Rev. D **23**, 347 (1981)
- [12] N. Balcall, J.P. Ostriker, S. Perlmutter, and P.J. Steinhardt, Science **284**, 1481-1488, (1999); C. Arnedariz-Picon, V. Mukhanov, and P.J. Steinhardt, Phys.Rev.Lett. **85**, 4438 (2000); K. Maeda, astro-ph/0012313; V. Sahni, astro-ph/0202076; D. Huterer, astro-ph/0202256.
- [13] J. K. Webb, M. T. Murphy, V. A. Flambaum, J. D. Dzuba, J. D. Barrow, C. W. Churchill, J. X. Prochaska, and A. M. Wolfe, Phys. Rev. Lett. **87**, 09130 (2001).
- [14] J. L. Martinez-Ledesma and S. Mendoza, astro-ph/0210444
- [15] D. Tytler, S. Burles, L. Lu, X-M, Fan, A. Wolfe, and B. Savage, AJ, **117** (1999) 63; F. C. van den Bosch, A. Burkert, and R. A. Swaters, astro-ph/0105082
- [16] R. H. Bradenberger, astro-ph/0208103
- [17] B. Moore, Nature 370 (1994) 629
- [18] M. Milgrom, astro-ph/0207231, astro-ph/0112069; R. H. Sanders and S. McGaugh astro-ph/0204521
- [19] F. Combes, astro-ph/0206126
- [20] R. Barkana and A. Loeb, astro-ph/0209515
- [21] B. M. Tinsley and J. E. Gunn ApJ 203 (1976) 52
- [22] C. Conselice, astro-ph/0212219
- [23] B. M. Poggianti, astro-ph/0210233, S. F. Helsdon and T. J. Ponman, astro-ph/0212047
- [24] S. Leon, J. Braine, P. Duc, V. Charmandaris, and E. Brinks, astro-ph/0208494, astro-ph/0210014
- [25] M. Bonamente, M. Joy, and R. Liu, astro-ph/0211439
- [26] J. Einasto, G. Hutsi, M. Einasto, E. Saar, D. L. Tucher, V. Muller, P. Heinamaki, and S. S. Allam, astro-ph/0212312
- [27] M. J. West, astro-ph/9709289
- [28] P. Langacher, M. Luo, and A. Mann, Rev. Mod. Phys. **64** (1992) 87.
- [29] A. O. Barut and D. Chung, Lett. Nuovo Cimento 38 (1983) 225
- [30] SLD Collaboration, Phys. Rev. D50 (1994) 5580
- [31] L. Hall, R. Jaffe, J. Rosen 1985, Phys. Rep. 125 (1985) 105
- [32] C.P. Singh, Phys. Rev. D24 (1981) 2481; D. B. Lichtenberg Phys. Rev. D40 (1989) 3675
- [33] Particle data Group, K. Hagiware et al., Phys. Rev. D, 66 010001-1 (2002)
- [34] G.E. Brown, M. Rho, V. Vento, Phys Lett 97B (1980); G.E. Brown, Nucl. Phys. A374 (1982) 630
- [35] D. Akers, hep-ph/0303139, hep-ph/0303261